Astrophysics with Extraterrestrial Materials

Larry R. Nittler[1] and Fred Ciesla[2]

[1]Department of Terrestrial Magnetism, Carnegie Institution of Washington, Washington, DC 20015; email: lnittler@carnegiescience.edu

[2]Department of the Geophysical Sciences, University of Chicago, Chicago, Illinois 60637

Keywords

meteorites, isotopes, protoplanetary disks, stellar evolution, planet formation, galactic chemical evolution

Abstract

Extraterrestrial materials, including meteorites, interplanetary dust, and spacecraft-returned asteroidal and cometary samples, provide a record of the starting materials and early evolution of the Solar System. We review how laboratory analyses of these materials provide unique information, complementary to astronomical observations, about a wide variety of stellar, interstellar and protoplanetary processes. Presolar stardust grains retain the isotopic compositions of their stellar sources, mainly asymptotic giant branch stars and Type II supernovae. They serve as direct probes of nucleosynthetic and dust formation processes in stars, galactic chemical evolution, and interstellar dust processing. Extinct radioactivities suggest that the Sun's birth environment was decoupled from average galactic nucleosynthesis for some tens to hundreds of Myr but was enriched in short-lived isotopes from massive stellar winds or explosions shortly before or during formation of the Solar System. Radiometric dating of meteorite components tells us about the timing and duration over which solar nebula solids were assembled into the building blocks of the planets. Components of the most primitive meteoritical materials provide further detailed constraints on the formation, processing, and transport of material and associated timescales in the Sun's protoplanetary disk as well as in other forming planetary systems.

Contents

1. INTRODUCTION

The Solar System was born some 4.6 billion years ago from a collapsing molecular cloud core containing material that had been formed, processed, and reformed by eons of galactic and stellar evolution (**Figure 1**). Earth and other planets formed from a protoplanetary disk (or solar nebula) analogous to those from which young planetary systems are observed to be forming today. A record of the starting materials and early evolution of the Solar System can be found in the roughly 40,000 tons of material accreted onto Earth every year from space. This material comes in a range of sizes, from submillimeter-sized dust particles, which are the most abundant in number, to larger, but less frequent, boulders measuring tens of meters or more in size, such as the bolide that exploded over Chelyabinsk, Russia, in February 2013. The extraterrestrial materials in our collections have been traced back to a wide diversity of asteroids, comets, another planet (Mars), and our own Moon. Each particle that enters Earth's atmosphere provides an historical record of the origin and evolution of the body from which it originated.

The utility of these extraterrestrial samples comes from our ability to measure their physical and chemical properties in great detail in the laboratory, in particular our ability to determine their elemental, molecular, and isotopic compositions with high levels of precision. These properties allow us to classify the samples into different types and begin to understand the origin and evolution of their parent bodies. Objects with similar bulk compositions and isotopic ratios are generally grouped together and thought to have a common origin, and they may come from a single parent body. Differences in compositions or isotopic ratios, however, often indicate that two samples were exposed to different evolutionary histories, were formed in different environments, or were exposed to a different set of processes prior to their study in a laboratory.

Over the past few decades, our ability to study and characterize extraterrestrial samples at higher levels of precision and smaller spatial scales has improved dramatically. These measurements have revealed the diversity of bodies that exist in our Solar System on both planetary (approximately thousands of kilometers) and microscopic (approximately nanometer) scales. Furthermore, the large amounts of data we have collected and the insights gained from these studies allow us to
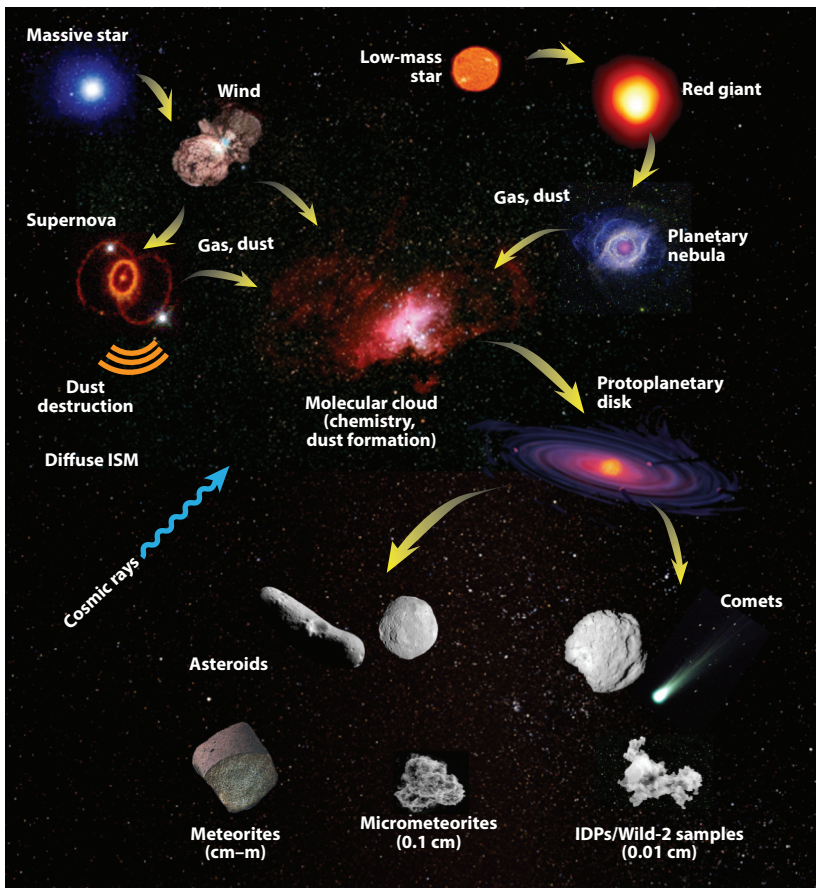
Figure 1

Connections between stellar, interstellar, and early planetary processes and extraterrestrial materials studied in terrestrial laboratories. Meteorites, micrometeorites, and IDPs are naturally delivered samples of asteroids and comets, which are remnants of planet formation in the Sun's protoplanetary disk. These samples contain records not only of planet formation processes, but also of presolar galactic, stellar, and interstellar processes. Images from NASA. Abbreviations: IDP, interplanetary dust particle; ISM, interstellar medium.

test and inform astrophysical models for the formation of the Solar System. Modern laboratory techniques provide vastly higher accuracy and precision for measurements of elemental and isotopic abundances and timescales than are achievable by astronomical methods. However, this is tempered by the fact that, despite the large volumes of data we have collected, the objects we have been able to study may be a limited or skewed sample of what exists in the Solar System. These materials are collected only after they have been liberated from their parent body in a collision or eruption, then nudged by the gravitational pull of the planets and radiation from the Sun onto Earth-crossing orbits. Even then, only a small fraction of such materials is accreted onto Earth and collected for study. Some parent bodies are better positioned than others to provide such materials, and thus must be aware of potential sampling biases. Nonetheless, these materials provide valuable insights into the processes that shaped our Solar System, and continued studies of these materials and collection of materials from known parent bodies will allow us to continue to develop and refine our understanding.

After a brief introduction to the various types of extraterrestrial materials available for study, this review illustrates how meteoritic studies provide unique information about a wide variety of astrophysical processes (**Figure 1**). Bona fide presolar materials, including dust condensed in prior generations of stars and extinct radioactive nuclei, reveal unique information about stellar and galactic processes and the astrophysical setting for Solar System birth (Sections 3–4). These materials along with the much larger amount of material formed within the Solar System enable us to probe the conditions and processes that occurred in solar nebula that eventually became our Solar System (Section 5). It is important to recognize that the study of extraterrestrial materials is very broad, and any review can provide only a selective sampling of the research that is ongoing at any point in time. More detailed reviews of many of the topics discussed here as well as ones we do not have room to address can be found in the literature (e.g., Beuther et al. 2014, Davis 2014).
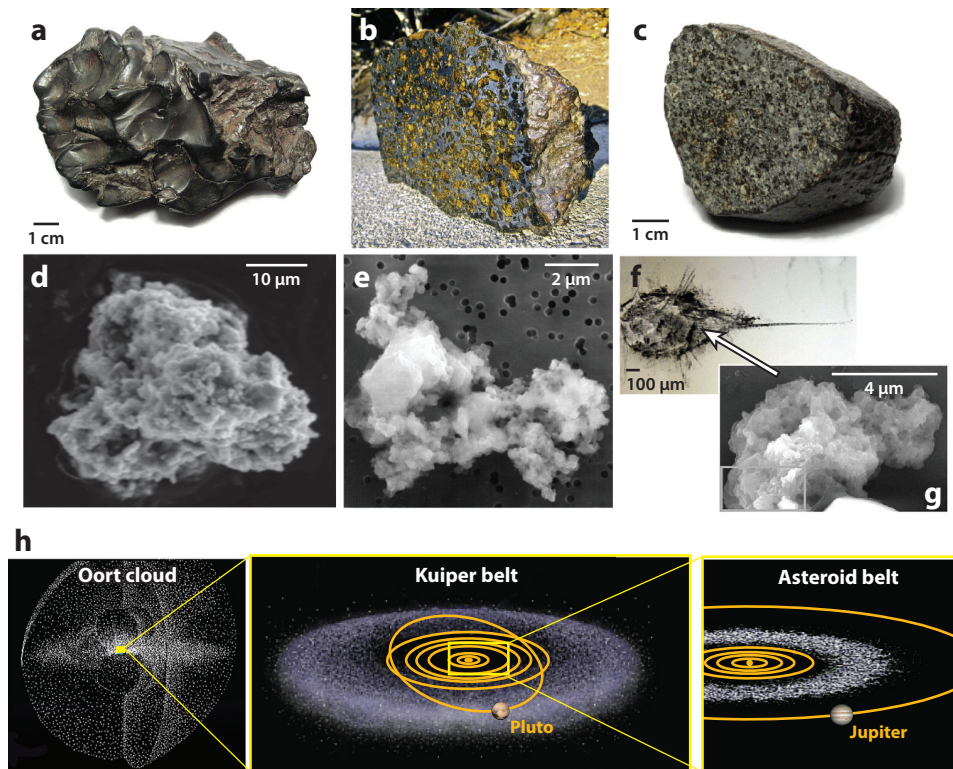
2. TYPES OF METEORITIC MATERIALS

The vast majority of knowledge on extraterrestrial materials has come from the study of meteorites, macroscopic (>1 mm) stones that have fallen from the sky and been recovered after landing. Although observed throughout human history, the nature of meteorite falls was controversial until the turn of the nineteenth century: A few prominent falls in Europe clearly established that rocks fall from the sky, thereby laying the groundwork for modern meteoritical science (e.g., Marvin 1995). Used since the 1960s to determine the trajectories of meteorites, photographic camera networks have shown that meteorites originate in the main asteroid belt between Mars and Jupiter. Although observed meteorite falls are of prime scientific importance because the samples are generally collected with minimal impact of weathering processes on Earth's surface, a large majority of meteorites available for study are "finds," largely from the cold and hot deserts of Antarctica and northern Africa, respectively. In many cases, the dry nature of these deserts allows for limited amounts of weathering, and glacially induced concentration mechanisms in Antarctica have allowed large numbers of meteorites to be found through systematic searches.

Although a common image of a meteorite in the popular imagination is that of a large block of metallic iron (Fe), iron meteorites, actually made of Fe-nickel (Ni) alloys, are relatively rare (6%) among meteorite falls (see **Figure 2** for examples of extraterrestrial materials). Most (93%) meteorites consist of rocky material (stony), and only ∼1% consist of roughly equal amounts of rocky material and Fe-Ni metal (stony-iron). Stony meteorites have been classified into a large number of groups and subgroups, but the most significant distinction is between chondrites and achondrites. Chondrites have bulk chemical compositions, excluding the most volatile elements, similar to that of the bulk Sun. They originate on asteroidal parent bodies that have not differentiated, e.g., that have not experienced melting and separation of an Fe-rich core from a rocky mantle and crust. Chondrites have been divided into many subtypes (see sidebar Chondrite Classification), based mainly on bulk elemental and isotopic compositions; these likely represent distinct parent asteroids with varied formation and evolutionary histories. Achondrites, by contrast, are mainly igneous rocks that clearly originated on differentiated bodies, including known bodies such as the asteroid Vesta, the Moon, and Mars.

The main focus of this review is chondritic meteorites, as these are the most primitive. That is, they contain a record of the earliest materials from the solar nebula, largely unmolested by subsequent processing on the rocks' parent asteroids. Chondrites have three major components (**Figure 3**):

1. Chondrules: small (typically 0.1–1 mm in diameter) spheres mainly composed of ferromagnesian silicate minerals. They clearly formed as molten or partially molten droplets that
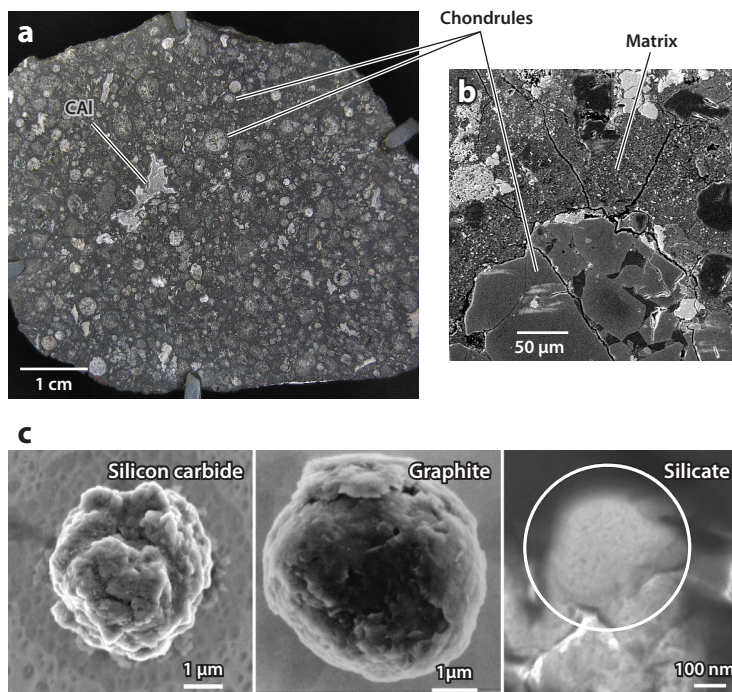
Figure 2

Types of extraterrestrial materials available for laboratory study. (*a*) Iron meteorite (Sikhote-Alin) (photo by H. Raab, licensed under CC BY-SA 3.0); (*b*) stony-iron meteorite (3-kg piece of Brahin pallasite) (photo by S. Jurvetson, licensed under CC BY 2.0); (*c*) stony meteorite (ordinary chondrite Northwest Africa 869) (photo by H. Raab, licensed under CC BY-SA 3.0); (*d*) AMM (courtesy of J. Duprat); (*e*) IDP (courtesy of NASA); (*f*) impact track in Stardust aerogel collector made by impacting comet Wild-2 particle; (*g*) close-up of one Wild-2 fragment from the Stardust aerogel track shown in panel *f* (Rotundi et al. 2008). (*h*) Solar System source regions of meteoritic materials: comets from the Oort Cloud (*left*) and Kuiper Belt (*middle*) are sources of many IDPs and possibly AMMs; most meteorites originate from the asteroid belt (*right*). Panels *a–c*, *f* are optical images, whereas panels *d*, *e*, and *g* are scanning electron micrographs. Abbreviations: AMM, Antarctic micrometeorite; IDP, interplanetary dust particle.

rapidly cooled and crystallized in space, but the setting and energy source for the heating is not known.

2. Refractory inclusions (RIs): less than millimeter- to centimeter-sized irregular inclusions of high-temperature minerals. One class of RIs, calcium-aluminum-rich inclusions (CAIs), has chemical and mineralogical compositions similar to those predicted for the first solids to form from a gas of solar composition as it cools and provides the oldest meteoritic samples dated by means of radiochronological methods. As such, they are used to define the age of the Solar System as a whole.

3. Matrix: a fine-grained (submicrometer to micrometer) collection of mineral and amorphous phases, packed between chondrules and RIs, that includes their broken-up fragments. Also in the matrix are trace amounts of isotopically anomalous presolar grains of stardust, tiny dust particles that originated in previous generations of stars (Sections 3–4), and organic

CHONDRITE CLASSIFICATION

Chondritic meteorites are subdivided into many groups based on shared chemical and isotopic characteristics, elemental composition, and physical properties such as the abundance and size of chondrules. Chondrites of a given group are presumed to have originated from the same or very similar parent asteroid(s). The majority of meteorite falls on Earth are ordinary chondrites (OCs), which are further divided into at least three groups according to Fe contents. Despite their name, carbonaceous chondrites (CCs) contain only up to a few percent of carbon (C). They are more rare but display more primitive characteristics than those of OCs. CCs are further divided into numerous subclasses, including CI (Ivuna type), CV (Vigarano type), CO (Ornans type), CM (Murray type), CR (Renazzo type), CK (Karoonda type), CB (Bencubbin type), and CH (high-metal type). Enstatite chondrites are chemically reduced compared with OCs and CCs, and Rumuruti chondrites are chemically similar to OCs but more oxidized. The remarkable diversity in physical and chemical properties of the different chondrite groups indicates that they sample a wide variety of environments and processes from the early Solar System.

Figure 3

(*a*) Photograph of slice of Allende carbonaceous chondrite with a calcium-aluminum-rich inclusion (CAI) and chondrules indicated (photo courtesy of Shiny Things, licensed under CC BY 2.0). (*b*) Scanning electron microscope image of Dominion Range 08006 carbonaceous chondrite, showing the fine-grained matrix that lies between CAIs and chondrules. Matrix includes trace amounts of presolar stardust grains that formed in outflows and ejecta of previous generations of stars. (*c*) Electron microscope images of three presolar grains (graphite image courtesy of Sachiko Amari; silicate image courtesy of Rhonda Stroud).

carbonaceous materials that possibly originated, at least in part, in the Sun's parental molecular cloud (Busemann et al. 2006).

Although undifferentiated, most chondrites have in fact experienced some degree of parent-body processing, for example, thermal metamorphism, where minerals are altered in composition and/or structure as a result of heating, and/or aqueous alteration, where mineral properties are modified through interaction with liquid water. Nonetheless, the most primitive meteorites, especially the carbonaceous chondrites, show very little evidence for either thermal or aqueous processing and are very valuable tools for astrophysics.

Beyond meteorites, additional types of extraterrestrial materials available for laboratory study include Antarctic micrometeorites (AMMs), interplanetary dust particles (IDPs), and spacecraft-returned samples. AMMs sample the peak in the size distribution of the flux of extraterrestrial materials on Earth, but measuring less than a few hundred micrometers, they are too small to be recovered as a meteorite falls. In fact, frictional heating on atmospheric entry destroys many of these objects (producing meteors or shooting stars), but some survive intact and can be recovered by melting and filtering Antarctic snow and ice. Less than 50 μm, IDPs are even smaller objects that are collected on special collectors deployed on the wings of aircraft flying high in the stratosphere. The collection altitude of 17 km is higher than terrestrial dust can generally be lofted. Thus, IDPs and solid particles of rocket exhaust dominate collected samples.

Both AMMs and IDPs can be further classified into hydrated and anhydrous samples. The hydrated particles contain clay-like minerals, similar to those seen in some types of carbonaceous chondrites and likely originated on asteroidal parent bodies. Anhydrous IDPs bear some similarity to the matrix found in those meteorites that show the least evidence for parent body alteration, but appear in many respects even more primitive: For example, they show higher abundances of C and N, higher porosity, and essentially no evidence of even limited thermal or aqueous alteration. These characteristics as well as dynamical arguments (Nesvorný et al. 2010) have led to the common assumption that anhydrous IDPs are largely cometary in origin and thus provide the opportunity to study different reservoirs of the solar nebula than those that are sampled by meteorites, although their small sizes and relative rarity provide technical challenges.

Spacecraft have returned three types of solid extraterrestrial materials to terrestrial laboratories for study. These include lunar samples brought by both the US Apollo and the Soviet Luna programs, dust from the Kuiper Belt comet (**Figure 2**) Wild-2 brought back by NASA's Stardust mission (Brownlee 2014), and dust from the surface of the near-Earth asteroid Itokawa brought by JAXA's Hayabusa mission (Nakamura et al. 2011). Another NASA sample-return mission, Genesis, retrieved solar wind atoms that had been implanted in high-purity materials (Burnett 2013). The Wild-2 samples show relationships both to IDPs and materials found in chondritic meteorites (e.g., CAI-like and chondrule-like objects). The Itokawa samples have confirmed the relationship between the most common type of meteorite fall (ordinary chondrites) and S-type asteroids, previously inferred from spectroscopic measurements, dynamical modeling, and NASA's Near Earth Asteroid Rendezvous mission to Eros (McCoy et al. 2002).

3. METEORITES AND STARS

3.1. Isotopic Anomalies and Presolar Stardust

Meteorites have long played a critical role in the development of our understanding of how the elements are synthesized in stars. For example, the observation of regularities in the Solar System elemental abundance pattern, defined by meteorite measurements, stimulated the development of the seminal work laying out the basic theory of stellar nucleosynthesis in the 1950s (Burbidge et al.

1957, Cameron 1957). Although numerous individual stars were well known to have contributed the metals, i.e., atoms heavier than helium (He), in the Solar System, researchers thought that the presolar material was thoroughly homogenized during the formation of the Solar System and only the average result of nucleosynthesis was preserved in the solar abundance pattern. However, starting with the discoveries of isotopically anomalous noble gases in the 1960s (Reynolds & Turner 1964) and anomalous O isotopes in CAIs in 1973 (Clayton et al. 1973), it became increasingly clear that the nebula contained primordial isotopic heterogeneities, linked at least in part to preserved presolar stellar material bearing the imprint of nuclear processes in individual stars. Here, an isotopic anomaly is defined as an isotopic ratio that cannot be derived from normal (average) solar system material via typical chemical or physical processes, for example, evaporation or diffusion.

In 1987, a long systematic search for the presolar carrier(s) of anomalous noble gases came to fruition with the discovery of individual grains of silicon carbide (SiC) and graphite with extreme isotopic anomalies in essentially all measured elements indicating that they are composed of pure stellar matter (Anders & Zinner 1993). Since then, numerous additional types of presolar stardust grains have been identified in extraterrestrial materials. Because these grains are essentially solidified pieces of individual stars at a given point in their evolution, they are powerful tools for probing processes of stellar evolution and nucleosynthesis, galactic chemical evolution, and dust formation in stellar environments, as illustrated below (see Zinner 2014 for a recent detailed review). Note that primitive extraterrestrial materials may also contain presolar dust grains with isotopic compositions similar to the Solar System, e.g., grains that formed in the protosolar molecular cloud (Section 4.1). Unfortunately, it is not currently clear how to identify such grains unambiguously, though constraining their abundance in some samples may be possible (Alexander et al. 2014).

In addition to the identification and study of individual preserved presolar grains, another type of presolar isotopic anomaly preserved in meteoritic materials and related to stellar processes is represented by radiogenic isotopic signatures indicating decay of radionuclides that were present at the formation of the Solar System. However, because their lifetimes are much shorter than 4.6 Gyr, they are now detectable only through their stable decay products; these extinct or short-lived radionuclides are discussed in Sections 4 and 5. Moreover, CAIs and bulk meteorites display isotopic variations of nucleosynthetic origin in a number of elements, implying heterogeneity in the distribution of presolar carriers of different isotopic signatures in the solar nebula (Section 5).

3.2. Types of Presolar Stardust Grains

The 1987 discovery of presolar carbonaceous stardust like SiC and graphite was made possible by the chemically resistant nature of these phases, the lack of a large isotopically normal background of such phases in meteorites, the fact that the grains contained isotopically anomalous noble gases, and the development of secondary ion mass spectrometry as a method for determining isotopic compositions of micrometer-sized dust particles. As a result, presolar grains could be purified by successive steps of acid dissolution ("burning down a haystack to find the needle") of the major mass of the meteorite samples. Since then, technological advances have allowed for the discovery of numerous additional types of presolar grains (**Figure 3**), both in meteoritic acid residues, e.g., refractory aluminum (Al) and magnesium (Mg) oxides and Si_3N_4, and in situ in meteorites, AMMs, IDPs, and comet Wild-2 dust. In particular, silicates are the most abundant class of presolar grains (up to a few hundred parts per million in the most primitive extraterrestrial materials compared to ∼30 ppm for SiC) but are acid soluble, and their discovery required the development of the high-sensitivity, high spatial resolution NanoSIMS instrument (a nano-secondary-ion mass spectrometry ion microprobe) by Cameca Instruments (Messenger et al. 2003). Some presolar phases, e.g., metallic Fe, titanium carbide (TiC), and molybdenum carbide (MoC), have been identified only as subgrains within larger presolar graphite and/or

silicate matrices and have important ramifications for how dust condenses in stellar environments (e.g., Bernatowicz et al. 1996). Note that nanometer-sized diamond crystals (nanodiamonds) were among the first reported types of presolar grains (Lewis et al. 1987). However, the origin of these grains is ambiguous (Dai et al. 2002), owing both to their tiny size and to the recognition that other phases are present in the nanodiamond-rich meteorite acid residues (Stroud et al. 2011).

3.3. Stellar Sources of Presolar Grains and Astrophysical Constraints from Presolar Grains

Every presolar stardust grain is a solid piece of stellar matter that condensed at a given place and time in a specific star. Because the actual parent stars have been dead for eons, comparison of measured isotopic compositions with astronomical observations and predictions of stellar evolution/nucleosynthesis models are required to identify the type of stellar source of a given grain (or class of isotopically similar grains). Analysis and interpretation of presolar grains require an iterative approach; once a stellar source for a grain is identified on the basis of one or more isotopic ratios, additional isotopic data can be used to refine models and improve understanding of processes within that type of star, or alternatively in some cases, these data indicate that the additional assignment of source was incorrect. The origin of some types of presolar grains (e.g., the $\sim$5% of SiC grains with $^{12}C/^{13}C$ ratios lower than 10) is still unresolved, largely owing to a lack of the theoretical understanding of potential sources. The classification and source identification of presolar O-rich grains and SiC grains are illustrated in **Figures 4b** and **5**, respectively. The ranges of isotopic compositions for materials that formed in the Solar System are indicated on the plots, underscoring the radically anomalous nature of the presolar grains. These plots can be considered analogous to the Hertzsprung-Russell diagram used to classify stars and identify subpopulations associated with different physical properties and stages of evolution. Examples of how these grains provide new astrophysical information about their sources are discussed below.

3.3.1. Asymptotic giant branch stardust.
As seen in **Figures 4b** and **5**, a majority of both O-rich and C-rich presolar grains in extraterrestrial materials (excluding the ambiguous nanodiamonds) are believed to have originated in asymptotic giant branch (AGB) stars, low- to intermediate-mass (1–8 $M_\odot$) stars in very late stages of evolution. The AGB phase follows the main sequence when the star is fueled by core hydrogen (H) burning, the Red Giant phase when the envelope composition is modified by the first dredge-up, mixing of deep material that experienced partial H burning, and the brief phase of core He burning. AGB stars are powered by alternately burning thin H and He shells that overlay an electron-degenerate core of C and O, which will eventually become a white dwarf remnant. These stars have large convective envelopes and strong mass-loss rates driven by condensation of dust in the cooling outer portions. Periodic mixing of material (third dredge-up) from the deep burning shells changes the envelope composition, mixing in freshly synthesized material, including ^{12}C and heavy elements made by the s-process (slow neutron capture) (Käppeler et al. 1990). Thus, although most or all stars start out with more O than C (O rich), the third dredge-up gradually increases the C/O ratio until it exceeds unity (C rich). This has a profound effect on dust chemistry: When C/O < 1, diagnostic infrared emission features indicate O-rich phases such as silicates and oxides are present, whereas in AGB stars with C/O > 1, observations indicate the presence of phases such as SiC and elemental C.

Because AGB stars are the primary producers of C and s-process elements in the Universe and also prodigious producers of dust to the interstellar medium (ISM) (Kemper et al. 2004), they are of great astrophysical importance, and presolar grain studies provide important information on a range of relevant astrophysical issues. For example, whereas most presolar O-rich grains
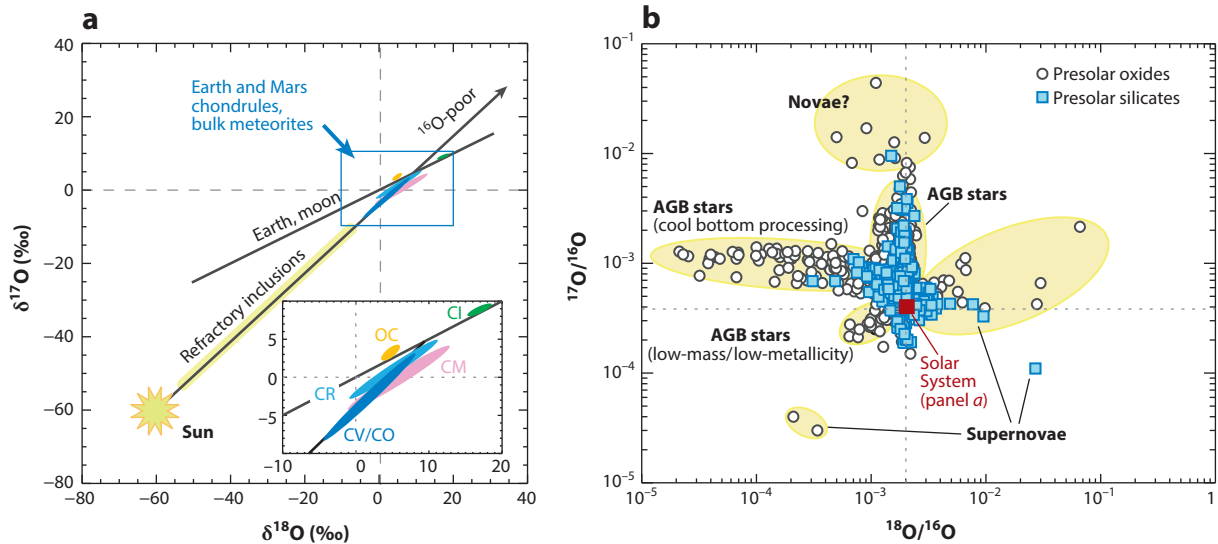
Figure 4

Oxygen isotopes in meteorites. (*a*) Schematic diagram of oxygen isotope ratio variations in the Solar System, expressed as δ-values, parts-per-thousand deviations from Earth's ocean water at 0,0. Compared with the Sun, bulk planetary materials have O-isotopic compositions similar to Earth, depleted in ^{16}O by ~6% (McKeegan et al. 2011). Refractory inclusions and some chondrules in meteorites are also enriched in ^{16}O, relative to Earth. Black arrow points toward rare ^{16}O-poor meteoritic grains with $\delta^{17}O \approx \delta^{18}O \approx$ +200‰ (Sakamoto et al. 2007). (*Inset*) Small isotopic differences are observed among different meteorite groups, making O isotopes a highly useful classification tool (see the sidebar Chondrite Classification). (*b*) O-isotopic ratios measured in presolar oxide and silicate grains (Nittler et al. 2008, Zinner 2014 and references therein); the range of panel *a* is indicated by the red rectangle. The ratios span enormous ranges and fall into groupings reflecting different nuclear processes in their parent stars. Inferred types of stellar sources are indicated; the vast majority of grains originated in AGB stars. Abbreviations: AGB, asymptotic giant branch; CI, Ivuna-type carbonaceous chondrite subgroup; CM, Murray-type carbonaceous chondrite subgroup; CR, Renazzo-type carbonaceous chondrite subgroup; CV/CO, Vigarano/Ornans-type carbonaceous chondrite subgroup; OC, ordinary chondrites.

(**Figure 4*b***) have O isotope ratios consistent with observations (Smith & Lambert 1990) and expectations for AGB stars (set by the first dredge-up of material affected by the CNO cycles of H burning) (Boothroyd & Sackmann 1999), one class of grains has much lower $^{18}O/^{16}O$ ratios than predicted by standard models. The best explanation of this observation, along with the unusually high abundances of radioactive ^{26}Al inferred in these grains from excesses of the decay product ^{26}Mg, asserts that the grains originated in stars that underwent an additional mixing process, cool-bottom processing, that is not predicted by standard AGB evolutionary models (Wasserburg et al. 1995, Nollett et al. 2003). Moreover, consideration of C, N, and Si isotopes in many presolar SiC grains indicates that this mixing also occurs in C-rich AGB stars (Nittler & Alexander 2003, Palmerini et al. 2011). Although some astronomical observations already implied this mixing, high-precision grain data provide constraints on model parameters, such as mixing rates and temperatures experienced by the mixed materials, that may help elucidate the still unknown physical mechanism(s) for the process (Nollett et al. 2003, Palmerini et al. 2011). For example, one popular proposed mixing mechanism, known as thermohaline diffusion, cannot explain the high inferred $^{26}Al/^{27}Al$ ratios observed in ^{18}O-poor grains, whereas other mechanisms including circulation driven by magnetic buoyancy (Busso et al. 2007, Nucci & Busso 2014) or internal gravity waves (Denissenkov & Tout 2003) remain promising.
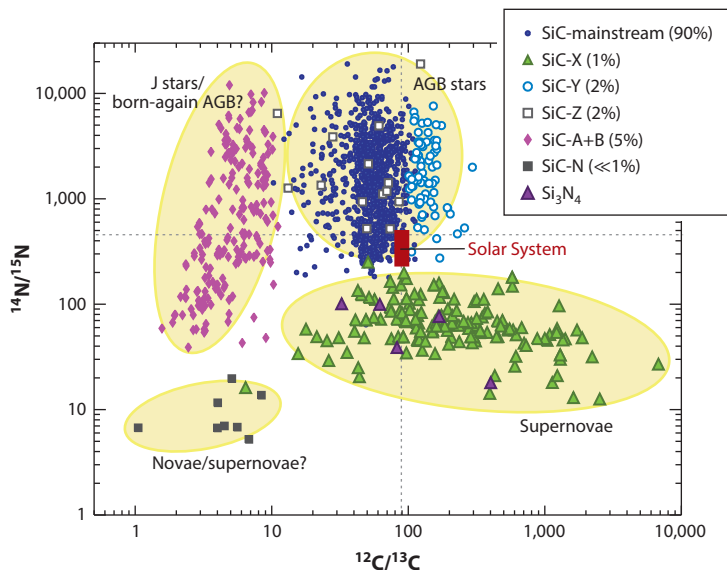
Figure 5

Carbon and nitrogen isotopic ratios measured in presolar SiC and Si_3N_4 grains (Zinner 2014 and references therein). As in **Figure 3b**, the data lie in distinct regions of the plot, reflecting different nuclear processes and stellar sources as indicated. The ranges of C- and N-isotope ratios in materials of known solar system origin are indicated by the red rectangle. Abbreviation: AGB, asymptomatic giant branch.

Of particular importance to understanding AGB star nucleosynthesis have been studies of heavy-trace-element isotopic compositions in presolar SiC grains (Lugaro et al. 2003, Savina et al. 2004, Liu et al. 2014b). In particular, measurements of Mo, zirconium (Zr), ruthenium (Ru), strontium (Sr), barium (Ba), neon, hafnium, tungsten (W), and lead in single grains whose major-element compositions point to an AGB origin have revealed mostly pure *s*-process isotopic signatures. This is profoundly important in confirming that the *s*-process is a real nuclear process that occurs in nature (it was originally identified on the basis of a mathematical deconvolution of the solar isotopic abundance pattern) (e.g., Burbidge et al. 1957). Moreover, high-precision laboratory data allow still uncertain AGB stellar models to be tested with a level of detail and precision simply not available from remote astronomical observations. For example, *s*-process nucleosynthesis occurs in AGB stars in the He-rich intershell region between He- and H-burning shells, where seed neutrons arise from the $^{13}C(\alpha,n)^{16}O$ reaction (Gallino et al. 1998, Cristallo et al. 2011). The predicted nucleosynthesis thus depends critically on the amount and distribution of ^{13}C present in the intershell region (the ^{13}C pocket), but these are free parameters in some calculations or derive from specific mixing assumptions in others. Presolar SiC data have been used with considerable success to provide constraints on the ^{13}C pocket (Lugaro et al. 2003). For example, Liu et al. (2014a, 2014b) recently showed that both Ba and Zr data for single SiC grains support a flatter distribution of ^{13}C across the intershell region than does the more typically assumed profile that decreases with depth. In some cases, SiC data have also pointed to deficiencies in the laboratory nuclear physics data that inform nucleosynthesis calculations (Voss et al. 1994, Koehler et al. 2008). Not only can grain isotopic signatures constrain nucleosynthesis processes, comparing models and data can also help narrow down the characteristics of parent stars. For example, AGB model calculations show that the details of nuclear reaction pathways depend

on stellar parameters like mass and metallicity (abundance of elements heavier than He). Thus, comparison of multi-isotopic-ratio data and model predictions has indicated that most presolar SiC grains originated in stars of relatively low mass ($\sim$2–3 $M_\odot$) and close-to-solar metallicity (Lugaro et al. 2003).

Although isotopic compositions of presolar stardust grains are crucial both for identifying and using these grains as tools to study stellar evolution and nucleosynthesis, additional important astrophysical information is encoded in their physical and chemical properties. Models of dust formation in circumstellar outflows (e.g., Gail & Sedlmayr 1999, Höfner 2008) predict the specific phases that form and their properties (size, degree of crystallinity, etc.). Astronomical observations also get at the same problem through analysis of spectral features related to dust (Speck et al. 1997, Henning 2010, Jones et al. 2012). Presolar grains provide ground truth for both models and observations and provide unique insights into stellar dust production. Largely through the use of techniques based on transmission electron microscopy (TEM), the microstructural and chemical characteristics of many grains of various types of AGB stardust have now been investigated. For example, a detailed TEM study of hundreds of presolar SiC grains (Daulton et al. 2002), the vast majority of which formed in AGB stars, found that only the two structures that form at the lowest temperature are present among the presolar AGB stardust, even though these grains can be synthesized in the laboratory with more than 100 distinct crystal structures (polytypes). The formation temperatures of these polytypes are consistent with expectations for C-rich AGB outflows, and the data place some constraints on where in the stellar atmospheres the grains formed. Pioneering work by Bernatowicz et al. (1996) found that many presolar graphite grains from AGB stars commonly contain tiny (tens of nanometers in size) subgrains of other phases, including Ti-, Ru-, Mo-, and Zr-rich carbides. Moreover, many grains are not pure graphite, but rather consist of nanocrystalline C cores surrounded by onion-like layers of crystalline graphite. The presence of internal subgrains enriched in s-process elements like Mo and Zr supports an AGB origin for these grains (Croat et al. 2005). Moreover, the physical characteristics of the graphites and their subgrains, through kinetic and/or thermodynamic equilibrium modeling, allow for constraints to be made on the properties of the gas from which they formed (e.g., C/O ratio, gas density) as well as the timescales for dust formation. A key result of such modeling efforts (Bernatowicz et al. 1996, 2005) is that gas densities required to condense the grains are much higher than astronomical observations had inferred for C-rich AGB stars. Because the latter are determined under the assumption of spherically symmetric outflows, the most likely conclusions from the graphite grains are that AGB star outflows are clumpy and the grains form in regions of relatively high gas density.

In the past decade, TEM methods have been used to analyze an increasing number of O-rich AGB stardust grains, including refractory oxides like Al_2O_3, $CaAl_{12}O_{19}$, and $MgAl_2O_4$ as well as approximately 50 silicate grains. The oxides are usually single crystals with crystal structures and compositions expected from equilibrium condensation from a cooling AGB envelope. This implies that the highest-temperature dust grains in AGB stars condense under conditions close to thermodynamic equilibrium, which is generally consistent with the SiC results of Daulton et al. (2002). However, the presence of phases not predicted by equilibrium condensation (e.g., Fe oxides) (Floss et al. 2008, Zega et al. 2015) and nonstoichiometric compositions of some grains (Zega et al. 2014) also indicate nonequilibrium formation processes. Although some astronomical spectra have been interpreted as implying that Al_2O_3 in AGB stars is predominantly amorphous (Jones et al. 2014), of the $\sim$10 presolar Al_2O_3 grains studied (Stroud et al. 2004a, Takigawa et al. 2014), only one was amorphous (Stroud et al. 2004a).

In contrast to the oxides, presolar silicates (the dominant class of dust in O-rich AGB stars, the ISM, and the presolar grain population) show a dizzying range of microstructures and compositions, including single crystals of Mg-rich olivine (Mg_2SiO_4) and pyroxene ($MgSiO_3$), compound

grains of multiple minerals (including silicate/oxide aggregates), mostly amorphous grains with patches of crystallinity, purely amorphous grains with nonstoichiometric compositions that are sometimes spatially heterogeneous on a scale of tens of nanometers, and others (Messenger et al. 2005; Nguyen et al. 2007, 2010; Vollmer et al. 2007, 2009, 2013; Keller & Messenger 2011; Stroud et al. 2013, 2014). The data set is still fairly limited, and significant biases may affect the survival of different phases relative to each other during the long journey of the grains from their parent stars, through the formation of the solar nebula and incorporation into asteroids and comets. These difficulties notwithstanding, some general conclusions can be drawn from the data:

1. AGB stars clearly produce a wide range of silicate phases, likely under both equilibrium and nonequilibrium conditions. There is no obvious preference for a single dominant phase.
2. Olivine is more common by a factor of 2–3 than is pyroxene in the presolar silicate population. This is consistent with astronomical evidence that AGB stars in the Milky Way produce more olivine than pyroxene, though pyroxene appears to dominate at lower metallicity (Jones et al. 2012).
3. Some presolar silicates contain Fe, in contrast to expectations from equilibrium thermodynamics, again pointing to nonequilibrium condensation processes in AGB outflows.
4. On the basis of TEM results reported to date, the fraction of crystalline presolar AGB silicates is ∼40%, slightly higher than estimates of 10–20% for AGB stars (Kemper et al. 2004), suggesting some survival bias of crystals over amorphous grains.
5. Although most presolar silicates are submicrometer in size (200–300 nm in diameter), the size distribution extends to >1 μm, indicating that conditions in AGB stars allow for the growth of large grains, consistent with some modeling and observational results (Höfner 2008, Norris et al. 2012).

3.3.2. Supernova stardust. Type II, or core-collapse, supernovae (SNe) are the explosive end-stage of the evolution of short-lived stars more massive than ≈8 $M_\odot$. Dust from Type II SNe has become a matter of considerable astrophysical interest in recent years with the observation of large quantities of dust in high-redshift galaxies that have not had time for AGB stars to evolve and produce significant amounts of dust (Pettini et al. 1994) and with the development of submillimeter telescopes like Herschel and ALMA that have detected large quantities of cold dust in SN remnants (Matsuura et al. 2011, Indebetouw et al. 2014). However, many fundamental questions of SN dust grains remain, including their compositions and sizes, how and where in the ejecta they form, and how they are processed by reverse shocks arising from interactions of the SN shock wave with the ambient medium. The existence of bona fide SN grains in meteoritic materials may help researchers answer such questions.

A small percentage of SiC, oxide, and silicate stardust grains and a larger fraction of presolar graphite grains have isotopic compositions clearly pointing to an origin in SNe (**Figures 4b** and **5**). The most diagnostic SN isotopic signature is the observation of large ^{44}Ca excesses unaccompanied by anomalies in other stable calcium (Ca) isotopes in many grains (Nittler et al. 1996). This signature points to in situ decay of ^{44}Ti, which has a half-life of ≈60 years and is produced solely in SNe. However, many other isotopic signatures in the grains also point to SN origins (Hoppe et al. 2000, Nittler et al. 2008, Amari et al. 2014), including evidence for very high levels of other now-decayed radionuclides including ^{26}Al, ^{41}K, ^{49}V, and the recently identified ^{32}Si (Pignatari et al. 2013b). The data are most consistent with an origin in Type II SNe, especially heavy-trace-element isotopic signatures (Meyer et al. 2000), though Type Ia SNe may explain some of the isotope data for SN SiC grains (Clayton et al. 1997).

It has been long argued, on the basis of a comparison of grain isotopic signatures with detailed calculations of nucleosynthesis in Type II SNe, that grain compositions require extensive, but

selective, mixing of material from different SN regions that experienced different nucleosynthetic histories (Travaglio et al. 1999, Hoppe et al. 2000). For example, ^{28}Si and ^{44}Ti excesses in many SN SiC and graphite grains require that material from very deep layers in the SN ejecta that experienced advanced nuclear burning stages be mixed with less-processed material further out that experienced only H or He burning, e.g., to explain high ^{26}Al/^{27}Al, ^{12}C/^{13}C, and ^{18}O/^{16}O ratios. This mixing must have occurred at a microscopic scale and must have avoided the very large quantity of ^{16}O present in the layers between the ^{28}Si-rich zone and the H- and He-burnt zones. Most O-rich presolar grains (**Figure 4b**) thought to have originated in SN have ^{18}O- and ^{17}O-rich signatures, best explained as mixtures of small amounts of material from inner zones (mainly the ^{18}O-rich He-rich layer, but also ^{24}Mg and ^{44}Ti from deeper layers) with larger contributions from the massive star's H-rich envelope (Nittler et al. 2008). Although exercises based on mixing variable portions of calculated SN zone compositions have been quite successful at explaining many of the broad features of the SN grain data sets, some discrepancies between SN models and the grain data remain puzzling, for example, SiC SN grains are both ^{15}N rich and ^{54}Fe poor relative to expectations from matching SN models to the other isotopic signatures in the grains (Hoppe et al. 2000, Marhas et al. 2008). Resolution of these puzzles is likely to improve our understanding of nuclear, mixing, and dust formation processes in SNe. The ^{15}N problem may be related to explosive H burning occurring at the base of the H-rich layer during the SN explosion (Lin et al. 2010, Meyer et al. 2011). Pignatari et al. (2013a) recently showed that many of the isotopic signatures of SN SiC and graphite grains could be explained by explosive He burning occurring in SNe with high shock velocities, as the shock heats the deepest He-shell material. In addition to relaxing the requirement of selective mixing, this scenario would also solve the ^{54}Fe problem, but it would not remove the need for mixing to explain the data for O-rich SN grains.

Advances in both astronomical observations and hydrodynamic modeling have improved our understanding of mixing in SN ejecta and generally support the conclusion that SN ejecta are heterogeneously mixed, but neither models nor observations yet address the microscopic scales required to explain the grain isotope data. Nonetheless, multidimensional numerical SN simulations indicate that Rayleigh-Taylor instabilities may cause fingers of deep material to penetrate outer zones, in rough accordance with the need to mix inner and outer material (Hammer et al. 2010, Joggerst et al. 2010). To avoid the difficult problem of selective mixing, Clayton and coworkers have advocated the formation of presolar SN SiC and graphite grains in O-rich layers of Type II SNe where radiation (especially Compton electrons) may dissociate CO molecules, thus freeing C to grow into large grains (Clayton et al. 1999, Clayton et al. 2001, Deneault et al. 2003, Clayton 2013). However, the isotopic compositions expected from this picture are inconsistent with the presolar grain data (Lin et al. 2010). Thus, even if some grains form in SNe in the manner proposed by Clayton and coworkers, they do not seem to be the same ones that are isolated from meteorites.

Just as with AGB stardust, the microstructural and mineralogical characteristics of SN grains provide ground truth for dust formation processes in SNe. Although microstructural studies of presolar oxides and silicates from SNe are relatively limited, the data thus far indicate characteristics that are mostly similar to those of grains from AGB stars (Messenger et al. 2003, Nguyen et al. 2011, Zega et al. 2011). In contrast, the structures of SN SiC and graphite grains show important differences from the same phases originating in AGB stars. For example, whereas AGB SiC grains are typically single crystals (often with many lattice defects), SN SiC and Si_3N_4 grains are more commonly aggregates of numerous small crystals (Stroud et al. 2004b, 2006; Hynes et al. 2010). Like AGB graphite grains, SN graphites (Croat et al. 2003) often have TiC subgrains, but the compositions of other subgrains are different (e.g., Fe, Ni metal, or osmium-rich grains rather than s-process-enriched carbides). Moreover, these subgrains often also have isotopic compositions
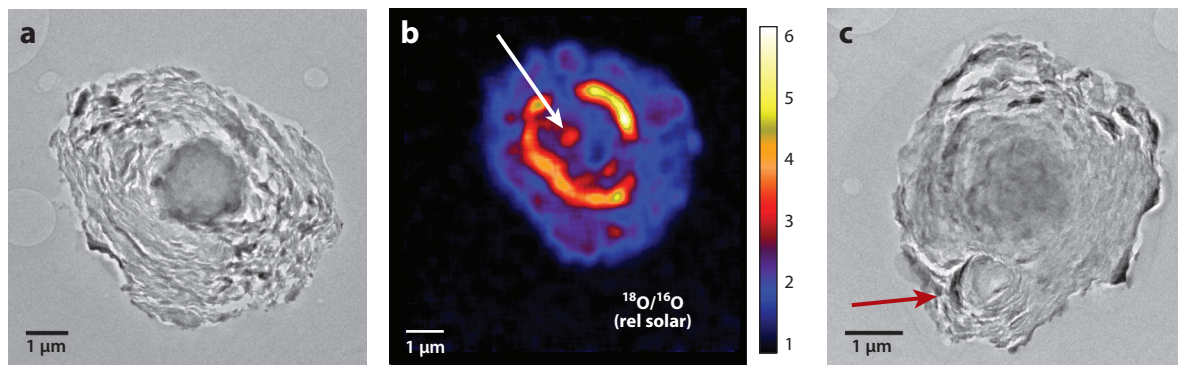
Figure 6

Slices of a presolar graphite grain from a Type II supernova (Groopman et al. 2014). (*a*) Transmission electron micrograph (TEM) of grain slice showing nanocrystalline core surrounded by layers of graphitized C. (*b*) O-isotopic ratio map of slice from panel *a*, expressed relative to the solar $^{18}O/^{16}O$ ratio of 0.002 (rel solar). The $^{18}O/^{16}O$ ratio varies dramatically across the grain, likely reflecting a change in gas composition in the supernova ejecta as the grain grew; an additional ^{18}O-rich hot spot (*white arrow*) corresponds to a TiC subgrain. (*c*) TEM of another slice showing a distinct micrometer-sized grain captured by the larger grain during grain growth (*red arrow*). Images courtesy of Evan Groopman.

distinct from each other and/or the host graphite (Stadermann et al. 2005, Groopman et al. 2012) and often show signs of having been ion irradiated (Croat et al. 2003). These observations indicate that the subgrains condensed independently from the graphites, perhaps in different parts of the SN ejecta, and were subsequently captured by the growing graphite grains. The complexity of many SN graphites is illustrated in **Figure 6**, which shows TEM and isotopic images for slices of a graphite grain extracted from the Orgueil CI (Ivuna type) carbonaceous chondrite meteorite (Groopman et al. 2014). This grain has a nanocrystalline core surrounded by layers of graphitized C. A striking feature is the observation that one of the graphitic layers is highly enriched in ^{18}O relative to the other layers, forming a bright ring in the isotopic ratio map of **Figure 6b**. Remarkably, as this grain grew, it also incorporated a separate smaller graphite spherule that had independently condensed (**Figure 6c**). The heterogeneous isotopic distribution and microstructures of this grain strongly indicate changing composition and/or physicochemical conditions during the condensation of the overall graphite grain as a result of fine-scale mixing of the ejecta and/or transport of the forming gain through ejecta with varying composition and conditions. Elemental heterogeneity observed across some SN SiC grains also points to changing conditions (e.g., temperature and/or gas composition) during grain formation (Nittler et al. 2007).

In sum, observations of SN presolar grains indicate that grain formation in SNe involves highly complex and dynamic processes. Observed differences between O-, C-, and N-rich SN phases may reflect differences in where the grains form within SN ejecta. As discussed above, the isotopic data for SN oxides and silicates are consistent with their being composed primarily of envelope material, whereas C-rich grains must have formed in deeper C-rich layers. The different microstructures suggest different conditions (e.g., gas density and temperature) for grains forming in different parts of the ejecta: The conditions for O-rich grains are somewhat similar to those in AGB outflows, whereas those for C-rich grains are strikingly different. The finely polycrystalline nature of one SN olivine grain (Messenger et al. 2005) supports this view, as this grain's composition rules out a significant envelope contribution and must have formed in deeper layers.

Given the discovery of large quantities of dust in SN ejecta, researchers speculate that SNe dominated stellar dust production in the early Galaxy and continue to do so even today (Indebetouw

et al. 2014). A fundamental question is how much of the dust that forms in SNe survives subsequent destruction by reverse shocks to then be injected into the ISM (Nozawa et al. 2007, Silvia et al. 2010, Biscaro & Cherchneff 2014). As discussed above, presolar SN grain compositions largely point to their being dominated by matter from outer portions of the ejecta (envelope as well as H- and He-burning zones) with only small contributions from the inner, most nuclear-processed zones. In particular, although ^{16}O is the most abundant isotope synthesized by Type II SNe and dominates much of the inner regions of SN ejecta (Rauscher et al. 2002), only two ^{16}O-rich presolar oxides have been identified, whereas the vast majority of identified O-rich SN dust are ^{18}O rich (**Figure 4b**). Observations indicate dust formation in deeper O-rich layers of SN ejecta (Rho et al. 2008), so the apparent dominance of grains from outer SN regions among the presolar grain data set suggests that reverse shocks are indeed highly destructive to newly formed dust in deep SN interiors, and thus SNe likely do not dominate dust production in the Galaxy.

Finally, a key observation of presolar SN grain studies is the demonstration that SN dust grains can be very large by usual astronomical dust standards. For example, although most presolar SiC grains from both AGB stars and SNe are submicrometer in size, the grain size distribution extends to tens of micrometers in diameter (Zinner et al. 2011), as do the sizes of presolar graphites. Large (>1 μm) dust grains have recently been observed to form rapidly in the ejecta of an SN (Gall et al. 2014), lending astronomical support to the conclusion that the large sizes of presolar SN grains are not unusual. Conversely, recent identification of <100-nm oxide grains with large ^{54}Cr (chromium) excesses (Dauphas et al. 2010, Qin et al. 2011) points to the formation of very small grains as well, though reliable O-isotopic measurements are not yet available for these grains.

3.3.3. Other stellar sources of meteoritic stardust.

Although AGB stars and SNe are implicated in the origin of most presolar grains, the isotopic compositions of some grains do not match expectations for either source and instead point to other origins. The most abundant are the so-called A and B subtypes of presolar SiC (**Figure 5**), which have $^{12}C/^{13}C$ ratios lower than 10 and $^{14}N/^{15}N$ ratios ranging from ~50 to >10,000; some graphite grains also have similarly low $^{12}C/^{13}C$ ratios. This C-isotopic composition matches observations of one class of C-rich giant stars, the J stars (Abia & Isern 2000), as well as a rare class of objects typified by Sakurai's object (Asplund et al. 1999) and known as born-again AGB stars and classical novae. Although they make up 10–15% of C stars, J stars are not well understood. Most appear to be less evolved than C-rich AGB stars and do not show s-process enrichments expected for such objects. Possible origin scenarios often involve phenomena related to binary stars (e.g., mergers and/or mass transfer between companions) (Sengupta et al. 2013, Zhang & Jeffery 2013), but their evolutionary origin remains enigmatic. Interestingly, recent astronomical data (Hedrosa et al. 2013) indicate that they have a similar range of $^{14}N/^{15}N$ ratios to that observed in SiC A and B grains, the latter of which also make up a similar portion of the total SiC data set to the frequency of J stars among C-rich stars. These observations suggest a connection between at least some of the grains and J stars, but a lack of understanding of J stars hampers testing this connection. More recently, observations of large nuclear anomalies in Ca, Ti, and S in some graphite and SiC A and B grains have made born-again AGB stars an attractive source for at least some of the ^{13}C-rich grains (Amari et al. 2001b; Heck et al. 2007; Jadhav et al. 2008, 2013; Fujiya et al. 2013). These are post-AGB stars believed to be experiencing a very late thermal pulse in which ignition of the He-burning shell and subsequent ingestion of H lead to production of ^{13}C and neutron-rich isotopes of various elements (Herwig et al. 2011). Calculations of the nucleosynthesis accompanying this pulse are in very good agreement with some grain data (Fujiya et al. 2013, Jadhav et al. 2013), indicating that born-again AGB stars are likely sources for some (but not all) of the ^{13}C-rich grains. Isotopic data for a few of the ^{13}C-rich grains point to novae and/or SN sources (Savina et al. 2003, Jadhav

et al. 2008, Heck et al. 2009a), which further complicates the picture, though these seem to be rare occurrences. In any case, data clearly indicate a range of sources for these enigmatic grains, underscoring the importance of obtaining isotopic data for as many elements as possible on single grains both to pin down stellar origins and to provide constraints on the processes occurring in the sources.

Classical novae have been suggested as sources of a very small fraction (<1%) of presolar SiC, graphite, silicate, and oxide grains (Amari et al. 2001a, Gyngard et al. 2010b, Leitner et al. 2012), in addition to a few of the ^{13}C-rich grains just discussed (Heck et al. 2007). Novae are explosive outbursts on white dwarf stars due to accretion of H from a close binary main-sequence or evolved companion. Their nucleosynthesis is dominated by explosive H burning, and they are among the main sources of ^{13}C, ^{15}N, and ^{17}O in the Galaxy. Thus, putative nova SiC and graphite grains were identified on the basis of very low ^{12}C/^{13}C and ^{14}N/^{15}N ratios (**Figure 5**) as well as associated ^{30}Si excesses in some grains, also predicted by nova nucleosynthesis models (José et al. 2004). However, a nova origin for these grains is not unambiguous. Multielement isotopic signatures in several grains with nova-like C and N isotopes indicate an origin in SNe (Nittler & Hoppe 2005, Liu et al. 2016), and a mechanism for producing such C and N signatures in SNe has been recently suggested (Pignatari et al. 2015). Nonetheless, novae have also been proposed as sources for the small fraction of O-rich presolar grains with very high ^{17}O/^{16}O ratios ($\gtrsim 5 \times 10^{-3}$) (**Figure 4**). These ratios are higher than attainable in AGB stars or SNe (Boothroyd & Sackmann 1999, Rauscher et al. 2002, Gyngard et al. 2011) but are in the range of nova models; Si and Mg isotopes in a few grains further support a nova origin (Gyngard et al. 2010a, Leitner et al. 2012, Nguyen & Messenger 2014). However, comparisons of the observed isotopic signatures of both the O-rich and C-rich grains with models of nova nucleosynthesis indicate that the nova signatures must be greatly diluted with material of more normal isotopic composition prior to grain condensation. The binary companion accreting onto a white dwarf to produce the nova outburst is an obvious source of such unprocessed material, but how such dilution might occur prior to grain formation has not been explained.

4. METEORITES AND THE GALAXY

The Solar System formed 4.6 Gyr ago from an interstellar molecular cloud consisting of gas and dust produced throughout the previous ~8 Gyr of galactic history. Its composition thus reflects the overall history of the various materials that went into it, and through some meteoritic materials, it preserves a record of galactic and interstellar processes. For example, some isotopic compositions in the presolar stardust grains discussed in Section 3 reflect the starting compositions of their parent stars, which in turn are influenced by processes of galactic chemical evolution (GCE), the gradual evolution of the chemical and isotopic compositions of new stars.

Presolar grains were once interstellar dust particles and thus can provide clues to understanding the nature of interstellar dust and how it is processed. The meteoritic record also allows for the determination of the initial abundances of various radioactive elements in the Solar System. These can shed further light on both long-term GCE and interstellar mixing processes as well as on the immediate astrophysical context of Solar System birth (e.g., possible injection of SN material directly into the Sun's parental cloud or protoplanetary disk).

4.1. Interstellar Dust

All galaxies, even very young ones observed at high redshift, are very dusty environments. The properties of interstellar dust in the Milky Way are inferred via a wide range of astronomical

observations, which indicate that the dust is dominated by amorphous silicates and carbonaceous grains, with typical sizes smaller than a few hundred nanometers in diameter (Whittet 2002). The origin of the dust is uncertain and controversial. Observations clearly show that evolved stars (AGB stars, red supergiants, Type II SNe) inject dust and organic molecules into the ISM. However, the relative proportion of dust from the various sources is uncertain, especially because until recently there were few constraints on the amount of dust produced and injected into the ISM by SNe. Moreover, subsequent processing of the stardust, for example, sputtering or shattering induced by SN shock waves, is indicated by both theory and observations (Seab & Shull 1983, Jones et al. 1996). Many studies indicate that the timescale for dust destruction in the ISM is much shorter than the timescale of injection of fresh stardust, and this is commonly taken to mean that much of the observed dust forms directly in the ISM (Draine 1990, 2009). This conclusion is tempered by the large uncertainties involved in the various timescale estimates and by the lack of a compelling mechanism for producing dust with the observed properties in the interstellar environment (Jones & Nuth 2011). Nonetheless, stars inject a significant amount of rock-forming elements like Mg, Si, and Fe into the ISM in the form of gas (especially Fe, which is largely produced in Type Ia SNe, which have not been observed to produce any dust). Because other observations indicate that a very large fraction of such elements is depleted from the gas phase and hence condensed into grains, this finding provides independent evidence for direct formation of dust in the ISM. If such interstellar grains formed in the Sun's parental molecular cloud, they would likely be isotopically indistinguishable from Solar System materials and thus not easily identifiable as presolar grains, even if present in meteorites or interplanetary dust.

In terms of the original stellar sources of interstellar dust, meteoritic presolar grain data indicate a predominance of dust from relatively low-mass AGB stars ($<4\,M_\odot$), with at most 10–15% of grains coming from Type II SNe (Qin et al. 2011). Thus, the data do not support SNe being a dominant dust source in the Milky Way as suggested by some recent observations (Indebetouw et al. 2014). Though it is not surprising that many presolar grains originated in AGB stars, given that observations show them to be prodigious dust producers, one surprising result from the grain data is the lack of grains from more massive AGB stars ($\sim$4–8 $M_\odot$). Models of dust production from stars of different masses, coupled with GCE models, indicate that massive AGB stars should have contributed at least as many O-rich grains to the ISM at the time of Solar System birth as did low-mass stars (Zhukovska et al. 2008, Gail et al. 2009), yet none have been observed (Nittler 2009). One possible explanation for this discrepancy is that one or more assumptions undergirding the models is incorrect. For example, if the isotopic signatures predicted for massive AGB stars are incorrect, the grains present in the meteoritic data set may be indistinguishable from grains from lower-mass AGB stars. Alternatively, the lack of grains from massive AGB stars may point to special circumstances in the local history of the material that went into forming the Solar System (Nittler 2013).

Because the presolar stardust grains were bona fide interstellar grains between the time of their formation and ejection from their parent stars and their incorporation into planetary materials, they provide a direct sample of ancient interstellar dust for laboratory analysis. As mentioned above, the timescales for dust destruction in the ISM (or equivalently, dust lifetimes) are highly uncertain. Presolar grains potentially provide a method for directly measuring lifetimes, either through direct absolute age dating via radiochronological methods or through the measurement of cosmogenic isotopes produced by galactic cosmic-ray interactions with the grains while in the ISM. Absolute age measurements have been precluded thus far owing to the low abundance of relevant elements (e.g., uranium) in the grains coupled with their small sizes. Small grain sizes also make age determinations via cosmogenic nuclides difficult both because cosmogenic isotopes could escape from grains as a result of nuclear recoil (Ott & Begemann 2000) and because the overall abundance of the relevant isotopes is low. Nevertheless, model interstellar residence ages based on

both neon- and lithium-isotopic compositions have been reported for relatively large (more than a few micrometers) SiC grains (Gyngard et al. 2009, Heck et al. 2009b). The results indicate a wide range of ages, from $<10^7$ to $\sim 10^9$ years, generally consistent with model predictions (Jones et al. 1997), but like the models, this range is also subject to potentially severe systematic uncertainties.

Grain-grain collisions and ion irradiation may be major channels for ISM grain destruction caused by the acceleration of grains, relative both to each other and to ISM gas, by SN shocks. Both types of processes may in principle leave an imprint in the microstructure of a grain, and one goal of laboratory studies of presolar grains is to search for such signatures. For example, Takigawa et al. (2014) recently reported a presolar Al_2O_3 grain with a surface feature resembling an impact crater as well as internal subcrystal misorientations and nanometer-sized voids, all of which suggest shock processing. The most likely source of the shock is an interstellar collision with another grain. Ion irradiation may lead to a number of observable signatures in crystalline materials, including amorphization and the generation of specific types of defects in the crystal lattices (Zega et al. 2014). Such signatures have not yet been unambiguously identified in presolar grains, but the data set is still very limited.

4.2. Galactic Chemical Evolution

As the Galaxy evolves, successive generations of stars contribute newly synthesized nuclei to the ISM, resulting in GCE (Pagel 1997, Matteucci 2003). Thus, the starting composition of any given star, including the Sun, is determined by the entire galactic history of the material from which it formed. In addition to an overall increase of metallicity (fraction of elements heavier than He) with time, many elemental and isotopic ratios vary as a function of time and/or galactic location. For example, stars formed early in galactic history are enriched relative to younger stars in α-elements such as ^{16}O, ^{24}Mg, ^{28}Si, etc., which are efficiently synthesized in Type II SNe, compared with Fe, a large fraction of which is produced by Type Ia SNe on much longer timescales (McWilliam 1997). Similarly, many isotopic ratios such as $^{18}O/^{16}O$, $^{25}Mg/^{24}Mg$, $^{29}Si/^{28}Si$, etc., increase with time owing both to metallicity-dependent nucleosynthetic yields and to different timescales for different nucleosynthetic processes (Clayton 1988). Various astronomical constraints are used to test models of GCE (and to constrain the various physical parameters that inform them), including metallicity and abundance ratio trends with age, galactic gradients in elemental and/or isotopic abundances, radioactive isotope abundances, and the cumulative metallicity distribution of long-lived stars formed throughout galactic history. Meteorites provide complementary information on GCE processes by providing the reference Solar composition for the entire periodic table and through studies of the presolar grains and extinct radioactivities they contain.

4.2.1. Galactic chemical evolution and presolar stardust grains. As discussed in Section 3, most isotopic signatures in presolar stardust grains reflect nuclear processes that occurred in the parent stars. However, the overall chemical history of the Galaxy is imprinted on many of the grains as well (Nittler & Dauphas 2006). In particular, some isotopic ratios, for example, those of Si in AGB SiC grains, span a wider range than expected from nucleosynthesis and mixing in single stars and are instead interpreted as representing a range of starting compositions of parent stars, most likely reflecting GCE processes (Timmes & Clayton 1996, Nittler et al. 1997, Alexander & Nittler 1999, Nittler 2009). Because the lifetimes of stars depend strongly on their mass and the grains formed in stars with a range of masses, parent stars formed with initial compositions sampling billions of years of GCE (Nittler & Cowsik 1997). Grain compositions can thus in principle be used as high-precision tools to study GCE, for example, to constrain many details that influence chemical evolution, including nucleosynthetic yields, star formation rate, and stellar

mass functions (Timmes et al. 1995, Kobayashi et al. 2011) as well as the influence of heterogeneous mixing of stellar ejecta in the Galaxy (Lugaro et al. 1999).

In practice, interpreting presolar grain data in terms of specific GCE models is not always unambiguous. For example, most presolar SiC grains have $^{29}Si/^{28}Si$ ratios higher than the Sun, despite the prediction of simple GCE models that they should have lower ratios because parent stars formed prior to the Sun and this ratio is expected to increase with time in the Galaxy. Numerous hypotheses have been put forward to explain this discrepancy (Clayton 1997, Clayton & Timmes 1997, Alexander & Nittler 1999): Perhaps most intriguingly, Clayton (2003) suggested the grain compositions reflect the result of a merger of a dwarf galaxy (with low $^{29}Si/^{28}Si$) with the Milky Way disk (with high $^{29}Si/^{28}Si$) some 10^9 years before the formation of the Solar System. This model is consistent with several aspects of the presolar SiC data and warrants further investigation. Even without a full understanding of the isotopic distributions, presolar grains have provided useful information on GCE. For example, correlations in Si and Ti isotopes in SiC grains limit the degree of chemical heterogeneity produced by heterogeneous mixing of supernova ejecta in the ISM to be at the 1–2% level (Nittler 2005).

4.2.2. Galactic chemical evolution and short-lived radioactivities in the Solar System. Since the seminal discoveries yielding evidence of extinct ^{129}I, ^{244}Pu, and ^{26}Al in meteorites (Reynolds 1960, Podosek 1970, Lee et al. 1976), extensive studies have revealed the presence in the early Solar System of many radioactive isotopes with lifetimes far shorter than the age of the Solar System (see sidebar Radiogenic Isotopes) (Huss et al. 2009, Dauphas & Chaussidon 2011, Davis & McKeegan 2014). Determining the abundances of these short-lived radionuclides (SLRs) in meteoritic materials is experimentally quite challenging, and the field has been somewhat unsettled in recent years. For example, new experimental results have led to substantial downward revisions of the estimated initial abundances of ^{60}Fe and ^{41}Ca (Liu et al. 2012, Tang & Dauphas 2012). In some cases, radioactive lifetimes have also been revised (Rugel et al. 2009, Kinoshita et al. 2012). Nevertheless, SLR measurements are valuable for astrophysics because they provide information about the nucleosynthetic history of the material that went into the Solar System and because they encode age information, both for Galactic processes and early Solar System processes (Section 5). The abundances of radioactive nuclei at a given place and time in the Galaxy are a function of a balance between stellar production and nuclear decay as well as interstellar mixing processes (Tinsley 1977, 1980; Nittler & Dauphas 2006; Huss et al. 2009). On average, one expects GCE to lead to steady-state abundances of radioisotopes in the ISM that are proportional to mean

RADIOGENIC ISOTOPES

The well-defined timescales of nuclear decay make radioactive isotope systems the fundamental tool of geochronology. When applied to meteorites, long-lived systems, with half-lives longer than the age of the Solar System, provide the overall age of the Solar System at 4.568 Gyr (Bouvier & Wadhwa 2010) as well as the absolute ages of meteorite components. Commonly studied systems include the U-Pb and Pb-Pb systems (which use variations in Pb isotopic ratios due to the decay of ^{235}U and ^{238}U) and the ^{87}Rb-^{87}Sr system (half-life = 4.9×10^{10} years). Short-lived radioactivities (SLRs) with half-lives shorter than the Solar System's age are detected by the excesses of their daughter isotopes and provide both information on the origin of the Solar System (Sections 3 and 4) and relative age information for different meteoritic materials (Section 5). Some important examples include ^{26}Al (half-life = 7.2×10^5 years), ^{129}I (1.6×10^7 years), ^{60}Fe (2.6×10^6 years), ^{53}Mn (3.7×10^6 years), and ^{182}Hf (8.9×10^6 years) (for recent reviews, see Dauphas & Chaussidon 2011, Davis & McKeegan 2014).

lifetimes, but with potentially large deviations due to the heterogeneous nature of star formation. If a region (e.g., the molecular cloud that formed the Sun) is isolated from the injection of newly synthesized isotopes for a time comparable to the lifetimes of certain radioactive elements, its complement of those elements is likely lower than the average steady-state abundance, due to an enhancement of radioactive decay, relative to stellar production.

The initial Solar System abundances of most known SLRs normalized to stable isotopes and theoretical production ratios are plotted against mean lifetime in **Figure 7**. The data would lie along a single line if they followed the expected trend for steady-state GCE at the time of Solar System formation. All but two of the plotted isotopes lie below the model line, indicating some level of isolation of the solar source material from continuous stellar production of the isotopes. The simplest interpretation of such data is to presume that the source material was isolated from any new input of nucleosynthetic material for a fixed period of time, a free-decay interval (Schramm & Wasserburg 1970). For example, a free-decay interval of 10^8 years can reproduce the inferred abundance of ^{129}I in the early Solar System (**Figure 7**). In this model, one would not expect any SLRs with mean lives shorter than $\sim 10^7$ years to survive, indicating that SLRs with shorter
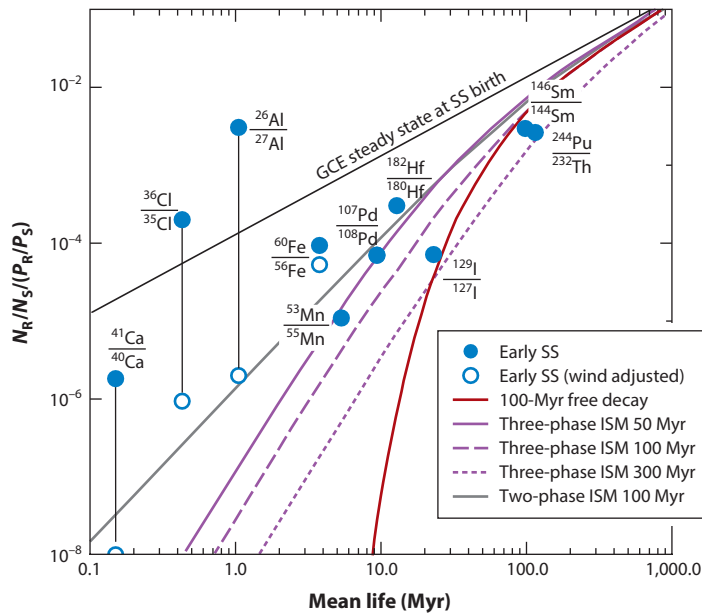
Figure 7

Short-lived (extinct) radionuclide/stable isotope (N_R/N_S) abundance ratios in the early SS, derived from meteorite measurements, plotted as a function of lifetime, and compared with predictions of theoretical models (after Huss et al. 2009, Young 2014). Y-axis values represent the inferred ratio at the time of SS formation, normalized to theoretical nucleosynthetic production ratios (P_R/P_S; see original references for details). Filled circles are based on standard nucleosynthetic yields, and open circles represent yields adjusted for production in Wolf-Rayet winds (Young 2014). The black line indicates the expectation for steady-state galactic evolution, whereas the curves indicate predictions for various models of ISM evolution: The red curve indicates a 10^8-year free-decay model, the purple curves indicate three-phase ISM models with mixing timescales (Huss et al. 2009), and the gray curve indicates a two-phase ISM model with molecular cloud residence time of 10^8 years (Young 2014). Abbreviations: Al, aluminum; Ca, calcium; Cl, chlorine; Fe, iron; GCE, galactic chemical evolution; Hf, hafnium; I, iodine; ISM, interstellar medium; Mn, manganese; Pd, palladium; Pu, plutonium; Sm, samarium; SS, Solar System; Th, thorium.

lifetimes require direct injection into the solar nebula by a stellar source (Wasserburg et al. 2006). However, more realistic GCE models (Clayton 1983, Jacobsen 2005, Huss et al. 2009) invoke mixing between different phases of the ISM (e.g., cold molecular clouds and hot diffuse ISM) and can better reproduce some of the data (**Figure 7**).

In either the free-decay picture or the more realistic multiphase ISM models, most SLR data suggest a decoupling of the material that formed the Solar System from the average GCE of the relevant radioisotopes for a timescale of tens to hundreds of millions of years. However, no single model explains all the data. One explanation, at least for longer-lived nuclides, is that the various isotopes are produced by different processes occurring on different timescales. Huss et al. (2009) discuss in detail the nucleosynthetic processes likely responsible for the various SLRs. Of particular interest are ^{129}I, ^{182}Hf, and ^{244}Pu, as all three have long been thought to be produced by the same general nuclear process (rapid neutron capture, or r-process) and thus might fall on a single curve as shown in **Figure 7**. This, however, is not observed: The early Solar System ^{182}Hf/^{180}Hf ratio is much higher than would be expected if ^{182}Hf was formed in the same r-process sources as ^{129}I. However, decades after the r-process nucleosynthetic process was identified, the astrophysical site or sites where it occurs remain unknown, though neutrino winds from SNe, low-mass SNe, mergers of neutron stars with each other or with black holes, and magnetorotationally driven SNe have all been suggested (Meyer 1994, Freiburghaus et al. 1999, Wanajo et al. 2011, Winteler et al. 2012). The discrepancy in ^{182}Hf and ^{129}I abundances in the early Solar System as well as elemental abundance measurements of ancient low-metallicity stars have led to the suggestion that there at least two different r-processes: one that produces r-process isotopes heavier than ~Ba and another that produces lighter r-process isotopes. If these processes occur on timescales different from each other, then the meteoritic data could be reconciled. However, Lugaro et al. (2014) recently showed that the major source of ^{182}Hf in the Universe is most likely intermediate-mass AGB stars, where it, along with ^{107}Pd, is produced by the s-process. This discovery removes one argument for separate sites for heavy and light r-process elements and provides some concordance for SLRs with lifetimes greater than ~9 Myr. That is, the abundances of ^{182}Hf and ^{107}Pd may reflect a mixing timescale of s-process material from AGB stars in the presolar Galaxy of a few tens of millions of years, whereas ^{244}Pu and ^{129}I indicate a longer timescale for r-process material. Samarium-146 is formed by the p-process (proton-capture or photodisintegration), another nucleosynthetic process whose astrophysical site is poorly understood. The concordance of ^{146}Sm with r-process nuclei ^{129}I and ^{244}Pu (shown in **Figure 7**) suggests a potential connection between the astrophysical sites of the r- and p-processes.

Molecular clouds have lifetimes of order 10^7 years, and SLRs with comparable or shorter mean lives may have abundances affected by processes connected to the Sun's parental cloud, for example, enrichment by SNe exploding in the cloud. A prime example is ^{26}Al (half-life = 720,000 years), which lies far above the expected galactic background at the time of Solar System formation. Almost 40 years ago, to explain this finding Cameron & Truran (1977) proposed that a SN shock wave both triggered the collapse of the protosolar cloud core into a solar system and directly injected freshly synthesized material. Although still a viable model supported by observations of triggered star formation (Preibisch et al. 2002), in the intervening years many additional ideas have been put forward to explain the relatively high abundances of ^{26}Al and other SLRs with lifetimes shorter than ~10 Myr. These can be divided roughly into the following three types of scenarios, all broadly considered self-enrichment in the sense that the nascent solar system is enriched in SLRs produced by stars that were born in the same molecular cloud: (*a*) triggered cloud collapse with concomitant direct injection of radioisotopes from a single SN or AGB star (Cameron & Truran 1977, Foster & Boss 1997, Boss & Keiser 2015), (*b*) direct injection of nuclei into an already-formed protoplanetary disk by a single SN (Ouellette et al. 2007, Liu 2014), and

(*c*) build-up of nuclides in a molecular cloud due to the formation and evolution of multiple massive stars that also contribute SLRs earlier in the history of the cloud complex (Gounelle et al. 2009, Gounelle & Meynet 2012). Recent work has also raised the question of the importance of injection from stellar winds versus from SN ejecta (Gaidos et al. 2009, Gounelle & Meynet 2012, Pan et al. 2012, Young 2014). Stars more massive than ~25 $M_\odot$ evolve through a Wolf-Rayet stage in which they lose huge amounts of material through winds enriched in some SLRs. Because winds and SN explosions will occur on different timescales and hydrodynamically interact differently with the molecular cloud material, some SLRs could decouple from each other (e.g., ^{26}Al and ^{60}Fe). Young (2014) recently advanced this idea and the build-up scenario by proposing a two-phase ISM mixing model in which Wolf-Rayet winds from massive stars, but not SN ejecta, get mixed into molecular clouds. He showed that early Solar System SLR abundances, when adjusted to take into account formation by massive star winds, are in reasonable agreement with the prediction of the two-phase ISM model (**Figure 7**).

Quantitative testing of these various scenarios is hampered both by severe uncertainties in crucial astrophysical aspects, such as nucleosynthetic yields and the details of hydrodynamic mixing of stellar ejecta into cold molecular material, and by changing estimates of SLR abundances in the early Solar System (Tang & Dauphas 2012). There is some evidence for temporally and/or spatially heterogeneous distributions of SLRs in the early Solar System. For example, rare meteoritic inclusions exhibit large nucleosynthetic isotopic anomalies in stable elements, suggesting they formed very early in the disk. However, they show no evidence for ^{26}Al (Davis & McKeegan 2014). These data are often interpreted as indicating relatively late injection of ^{26}Al, after these objects formed, thereby supporting the triggered cloud collapse or direct injection scenarios discussed above. Direct injection of SN ejecta into the protoplanetary disk may also be supported by Cr-isotopic variations in bulk meteorites and presolar grain abundance differences between comets and asteroids (Qin et al. 2011). In contrast, the model of Young (2014) disfavors injection scenarios but is based both on a highly simplified analytical model and on an assumption that Wolf-Rayet stars do not explode as SNe. The latter assumption is called into question by recent astronomical data (Gal-Yam et al. 2014). Although there is currently no consensus regarding the origin of the shortest-lived SLRs, meteorites will play a crucial role as researchers unravel the astrophysical context for the birth of our Solar System.

5. METEORITES AND THE PROTOPLANETARY DISK

The Solar System began to form 4.6 billion years ago upon gravitational collapse of a molecular cloud core that consisted primarily (~99% by mass) of molecular H and He, with trace amounts (~1% by mass) of dust grains, ices, and organics of the type discussed thus far. As collapse proceeded, much of the mass gathered in the center to form a young sun, while a fraction settled into orbit around the young star forming our protoplanetary disk, the solar nebula. Within the solar nebula, many of the interstellar solids contained within the nascent core were subjected to a series of dynamical, chemical, and thermal processes that led to their destruction or alteration. In some regions, new solids unlike those found in the ISM formed, as chemical environments within the solar nebula differed significantly from those found in circumstellar envelopes and molecular clouds. These new solids, along with those preserved from the ISM, eventually aggregated together over millions of years to form the planets, asteroids, and comets we see today.

Over the past few decades, astronomical observations enabled by new technologies and facilities have dramatically improved our understanding of how protoplanetary disks form and evolve as well as how dust is processed during the early stages of planet formation. However, such observations are somewhat limited because they reveal only the conditions and dust properties present at the

disk surface, whereas the optically thick midplane, the presumed site of planet formation, is hidden from view.

Asteroidal meteorites and IDPs provide a number of opportunities to study the conditions present and processes that operate within the otherwise hidden interior of a protoplanetary disk. Because these objects represent direct samples of the planetesimals (kilometer-scale, rocky building blocks of planets) that formed within our own protoplanetary disk, they provide constraints on the chemical and physical evolution of dust grains, dynamical mixing across the disk, and growth from submicrometer grains to kilometer-scale planetesimals. Such information can be combined with studies of the large-scale evolution of protoplanetary disks developed through astronomical observations to better understand this epoch of planet formation. Here we focus on key cosmochemical studies that have provided insights into the solar nebula epoch in the Solar System's history that would not have been possible without the study of extraterrestrial samples.

5.1. Dust Destruction and Alteration

Chondritic meteorites and IDPs provide the best clues for determining the physical and chemical properties of dust grains that were present within the solar nebula and that aggregated to form planetesimals. The extent to which these samples reflect all the materials from which planetesimals formed is uncertain, as heating and differentiation destroyed the original dust that formed the achondrite/iron meteorite parent bodies. However, because all chondritic meteorites share similar bulk characteristics, make up the largest portion of the extraterrestrial materials that fall to Earth, and have been spectroscopically linked to the dominant populations found in the asteroid belt, the different chondritic components may be representative of much of the dust found in the inner solar nebula, that is, the region where rocky asteroids and planetesimals formed.

5.1.1. Refractory inclusions. RIs (**Figure 3**), which include CAIs and amoeboid olivine aggregates, are so named because they contain the most refractory elements, that is, those that form solids at high temperatures. They are predominantly composed of Ca and Al oxides, Fe-Ni metal, and forsterite (Mg-rich olivine, Mg_2SiO_4), which thermodynamic calculations predict are the only major minerals present in a protoplanetary disk at temperatures in excess of 1,300–1,500 K (Grossman 1972, MacPherson et al. 1988, Ebel 2006). At lower temperatures, many of these minerals are not stable (particularly Ca and Al oxides, which dominate CAI mineralogy), and thus they would not form if temperatures did not exceed 1,300 K somewhere in the solar nebula. The presence of these Ca- and Al-rich minerals indicates very high temperatures were reached within the solar nebula, despite the absence of observational evidence for such high temperatures in protoplanetary disks (D'Alessio et al. 2005).

Temperatures this high may have existed early in the history of the solar nebula, particularly during and immediately after disk formation, as the release of gravitational potential energy from the natal molecular cloud and internal dissipation within the disk would be strongest at this time (e.g., Boss 1998, Yang & Ciesla 2012). As further detailed below, radiometric dating provides absolute and relative ages of these samples with precisions of order hundreds of thousands of years or less. In particular, application of the Pb-Pb and ^{26}Al systems shows that CAIs are the oldest objects to have formed in the solar nebula, predating other meteoritic materials by as much as 3–5 Myr (Amelin et al. 2002, Brennecka et al. 2010, Connelly et al. 2012). Given that the typical lifetime of a protoplanetary disk is of order ∼3 Myr (Haisch et al. 2001), this suggests that the highest temperatures recorded by protoplanetary dust come from the earliest epoch of disk evolution. Moreover, RIs are enriched in ^{16}O, relative to most other planetary materials (**Figure 4a**), similar to the inferred bulk isotopic composition of the Sun (McKeegan et al. 2011). Thus, these objects likely provide a record of the very early epoch of protoplanetary disk evolution,

in which high temperatures were present and chemical equilibrium, or a good approximation of equilibrium, was reached.

5.1.2. Chondrules.
Similar to RIs, chondrules (Section 2) provide evidence for high-temperature environments within the solar nebula. They are typically the most abundant component of chondritic meteorites, making up nearly 80% of the volume of the ordinary and enstatite chondrites, whereas their abundance can range from 0 to 70% in carbonaceous chondrites (e.g., Scott et al. 2005, Scott 2007). Their igneous textures along with their spherical shapes imply that they formed by crystallization of a melt. Peak temperatures of 1,700–2,400 K are needed to melt chondrules (Connolly & Desch 2004, Desch et al. 2012), a temperature range that again exceeds the temperatures typically expected or observationally inferred within protoplanetary disks. That such a major component of primitive bodies (along with some CAIs) formed from molten droplets has presented one of the major challenges to completing our understanding of the physical evolution of protoplanetary disks, as standard models do not include mechanisms that melt vast amounts of solids prior to planetesimal formation. That is, chondrules provide evidence of major melting events, yet such events would not have been predicted without their identification in the meteoritic record.

The event(s) that produced chondrules remain elusive, despite decades of petrologic studies and laboratory experiments dedicated to reproducing their textures, chemistry, and isotopic properties. As a result of these efforts, we know chondrule formation occurred in such a way to meet the following constraints (Desch et al. 2012):

1. Chondrule precursors, the dust that eventually melted to form chondrules, began at temperatures low enough for FeS to have formed ($T < 650$ K), as this mineral is found in the interior of chondrules. Higher ambient temperatures would have prevented FeS from forming.

2. Chondrule precursors were heated on timescales of seconds to minutes to temperatures of 1,700–2,100 K, at which point they were partially or completely melted. Temperatures lower than this would not have resulted in melting, and temperatures much higher than this would have resulted in rapid vaporization. Furthermore, slow heating would have led to vaporization of the precursors, as the condensation/vaporization point of the component minerals is ~1,300–1,500 K under protoplanetary disk conditions.

3. Upon reaching their peak temperatures, chondrules began to cool at rates of order 10–1,000 K/h during crystallization of the melts (in the temperature range ~1,400–1,800 K). Faster cooling would have resulted in glassy textures developing instead of the igneous textures that are observed, whereas slower cooling would have resulted in the devolatilization and fractionation of isotopes that are not observed (Alexander 2004, Davis et al. 2005, Alexander et al. 2008).

The cooling rates inferred for chondrules are particularly important because they provide information about the scale of the heating event and the environment where this event occurred. Cooling rates of 10–1,000 K/h are slow compared with the radiative cooling timescale of a single chondrule (at 1,500 K, a chondrule would cool at a rate of $\sim 10^6$ K/h if allowed to radiate to free space), suggesting that heating occurred in a sufficiently large and dusty volume to have trapped thermal energy and slow the loss of energy through mutual radiative heating. However, this cooling is rapid compared with the cooling timescale of the entire nebula, showing that heating must have been localized.

The above represents the zeroth-order picture for chondrule formation that has served as the framework for understanding these objects for decades. In recent years, further constraints on the environment where chondrules must have formed have been recognized. In particular, the isotopic

compositions of chondrules, especially for Na and K, show no mass-dependent fractionation, indicating that they did not lose these elements through evaporation into a vacuum or low-pressure environment (Cuzzi & Alexander 2006, Alexander et al. 2008, Hewins et al. 2012). This has been taken as evidence for formation in very-dust-rich environments, where the gas becomes saturated in Na and K by evaporation of a small fraction of solids, preventing further evaporation of the species remaining in the chondrules. The partial pressures required to saturate the gas in Na and K, however, are very high and indicate chondrule formation occurred in regions where solids were present at very high spatial densities, suggesting a dust-to-gas mass ratio of at least 10^5–10^6 times greater than that of a gas of solar composition (Alexander et al. 2008, Fedkin et al. 2012, Hewins et al. 2012). This is a very high concentration of solids, indicating that either the nebula was very efficient at concentrating dust in small volumes or that chondrule formation was tied to the presence or formation of planetesimals.

Multiple mechanisms have been suggested as being responsible for the rapid heating and proper cooling environment for chondrules. Over the past ~20 years, the shock-wave model has received a lot of support, as it has been studied in sufficient quantitative detail to demonstrate the possibility of producing thermal histories consistent with the constraints outlined above (see review by Desch et al. 2012 and references therein). This model posits that shock waves of some unspecified origin propagated through the solar nebula gas. In the undisturbed nebula, the gas and solids would be in thermal and kinetic equilibrium with one another (same temperature and no relative velocity with respect to one another). As a shock wave overruns a region of the nebula, the temperature and density of the gas increase while its velocity with respect to the shock decreases. Solids would initially be unaffected by the shock but would experience rapid energy and momentum exchange with the surrounding gas upon passing through the shock front. Via this exchange, the solids would be heated to high temperatures and would lose their relative velocity with respect to the gas. The entire system would then cool over long periods because the solids would have to radiate away not only their thermal energy, but also the thermal energy of the gas—the gas would provide a thermal reservoir that would keep temperature elevated for a long period of time.

More recently, attention has focused on determining the source of the shocks that could form chondrules. Though shocks are common in many astrophysical environments, the conditions needed to form chondrules are somewhat limited. That is, chondrule thermal histories would be achieved only from the proper combination of solar nebula gas densities and shock velocities. Because collisions between the gas and solids primarily serve to heat chondrules, these collisions must be frequent and energetic enough to reach the high temperatures required to melt chondrules but not too frequent and energetic to lead to their vaporization. For gas densities of 10^{-10}–10^{-8} g/cm³, appropriate for the midplane of the inner solar nebula, shock velocities of 7–10 km/s are required. Lower gas densities would require higher velocity shocks. Large shocks, >10^4 km in scale, were thought necessary to ensure that radiative cooling of the shocked region would occur on long enough timescales to match chondrule cooling rates. Although shocks could be produced within a gravitationally unstable disk, shocks that meet the necessary conditions to form chondrules are extremely rare (Boss & Durisen 2005, Boley & Durisen 2008). Stammler & Dullemond (2014) have also suggested that cooling of the postshock region in a large shock would be too slow for chondrules to retain volatiles. Instead, they argue for small-scale bow shocks such as those created by supersonic planetesimals or embryos in eccentric orbits in the solar nebula.

The additional constraint that chondrule formation must have taken place in very dust-rich environments has also proven to be a challenge for the shock-wave model. The original models that reproduced chondrule cooling rates only considered solid-to-gas mass ratios up to ~100 times that of a gas of solar composition, orders of magnitude below the values required to saturate the nebula in Na and K vapor. Higher solid densities lead to higher cooling rates, which would put the model

at odds with the constraints identified above. In response, some researchers have considered planetesimal and embryo bow shocks as sites for chondrule formation, where vapor from the surface of a hot planetesimal would saturate the gas in Na and K to prevent evaporation from hot chondrules during processing without the need for extreme chondrule densities (Morris et al. 2012). Detailed hydrodynamic simulations of such shocks, however, show that only very rapid cooling rates (>1,000 K/h) can be achieved and the conditions needed to match peak temperatures and marginally match cooling rates are limited to a small region of parameter space (Boley et al. 2013).

In part because of these issues and uncertainties, other models for chondrule formation have been explored in recent years. Specifically, regaining traction is an old idea that chondrules were formed as a result of collisions between young planetesimals. Asphaug et al. (2011) demonstrated that low-velocity (~1–100 m/s) collisions between molten planetesimals would liberate large amounts of melt into space. Johnson et al. (2015) proposed a different model that invoked high-speed collisions (>2.5 km/s) of planetesimals into larger embryos, demonstrating that shock heating could melt cold target material and eject this melt to space in a phenomenon called jetting (**Figure 8**). In both cases, the ejected melt, which originated in dense planetesimals, would be initially much more concentrated than the nebular dust, leading to relatively slow cooling. If this melt forms chondrule-sized spheres and expands slowly enough, proper cooling rates may be achieved (Dullemond et al. 2014, Johnson et al. 2015). Whether the suite of chemical and petrologic constraints can be met in the context of this model requires further study.

If chondrules formed as a result of impacts between planetesimals, the view of chondrule and chondritic meteorites as records of planet formation would need to shift dramatically: Rather than
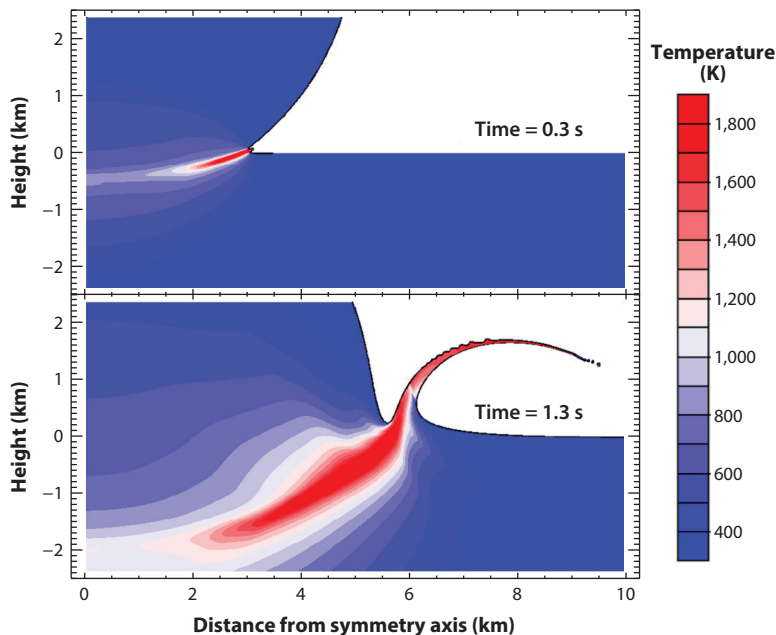
Figure 8

Model calculation results for jetting of molten material during the impact of a 10-km projectile on a larger target at 3 km/s; the collision site is at the origin (after Johnson et al. 2015). A jet is beginning to form at 0.8 s (*top*) and is fully formed at 1.3 s (*bottom*). Chondrules may plausibly form in such jets. Figure courtesy of Brandon Johnson.

being products of nebular processes, these objects would be the product of planetary processing. Thus, these materials would not be completely dominated by dust grains and processes that operated in the protoplanetary disk; instead, they would be the consequences of planetesimal dynamics and planetary accretion. That is, chondrites would not be fully representative of the original building blocks of planets.

5.1.3. Matrix. Even if chondrules were formed in secondary-type events, the matrix found in chondritic meteorites (**Figure 3**) is still largely expected to be representative of the fine dust that was present in the solar nebula. Chondrite matrices represent a mix of different materials and phases, including presolar grains (Section 3), volatile organics, and processed crystalline silicates. The issue of chondrule-matrix complementarity—that is, whether chondrules and bulk matrix differ in chemical properties but when added together produce approximately solar compositions— has been used to argue for genetic links between these two types of material (e.g., Palme et al. 2015). However, the presolar grains and organics found in matrices would not have survived had they been exposed to CAI- and chondrule-forming environments. These relatively fragile materials are intimately mixed with chondrules and CAIs on the centimeter scale within chondritic meteorites (**Figure 3**), indicating extensive mixing and sampling of different environments in the nebula— pointing to a dynamic nebula.

In summary, meteorites and the components they contain provide important insights into the environments and conditions that existed within the solar nebula. Although evidence for very high temperatures is not seen in astronomical observations of protoplanetary disks, the presence of chondrules and CAIs indicate that planetary materials were exposed to such temperatures during the first few million years of Solar System evolution. These materials are mixed with other minerals and components that could have survived only at low temperatures, indicating significant mixing and transport was occurring during the assembly of planetesimals. We discuss mixing and transport in the nebula in further detail below (Section 5.3).

5.2. Chronology of Disk Evolution and Planetesimal Accretion

Laboratory analyses of meteorites and their components have also revealed the relative and absolute timing of events during planet formation through the use of measurements of the decay products of radioactive isotopes (see sidebar Radiogenic Isotopes). With a half-life of $\sim$720,000 years, the ^{26}Al-^{26}Mg system provides the most precise relative ages of any radiometric system during the solar nebula epoch. Pb-Pb dating provides an absolute chronology of events, with precision that has improved dramatically over the past decade. Application of these systems to the individual components found in chondrites reveals that CAIs formed first in the solar nebula, in an environment with the highest ratio of ^{26}Al to ^{27}Al (where ^{27}Al is a stable isotope used to measure the relative abundance of the radioactive isotope), with typical (commonly referred to as canonical) values of ^{26}Al/^{27}Al $\sim 5.2 \times 10^{-5}$ in such objects (Lee et al. 1977, MacPherson et al. 1995, Jacobsen et al. 2008). Chondrules, however, have a range of ages: Some chondrules may have formed contemporaneously with RIs, whereas others, if not most, formed 2–3, and possibly up to 5, million years later (Amelin et al. 2002, Kita et al. 2005, Krot et al. 2005c, Connelly et al. 2012).

If chondrules are nebular products and are not formed by planetesimal collisions, then the reported ages provide important information about dust growth and the global evolution of the solar nebula. Because many chondrules are 2–3 Myr younger than CAIs, the solar nebula must have been present for at least this long. Such a disk lifetime is consistent with the inferred median lifetime of protoplanetary disks around other stars (Haisch et al. 2001). Furthermore, because chondrules would form from dusty precursors in this nebula, a substantial amount of dust or

dust aggregates was present within the nebula at this time. Again, this is consistent with the astronomically determined ages of disks, as these observations infer the presence of disks by measuring the flux of radiation from small dust grains. Indeed, because chondrite parent bodies could not fully predate the chondrules they contain, planetesimal formation must have been under way many millions of years into nebular evolution. A collection of precise chondrule ages from a range of meteorite types would help us determine how this dust population evolved over time.
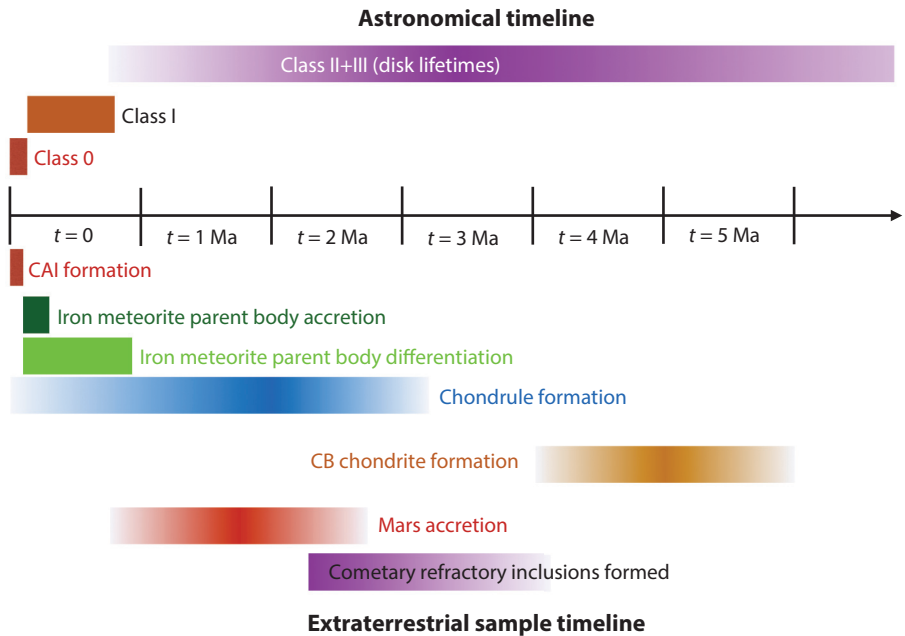
Whereas the prolonged formation of chondrites provides limits on the final stages of planetesimal formation, iron meteorites and achondrites (Section 2) provide important insights into when planetesimal formation began. Although the parent bodies for these meteorites have evolved as a result of melting and high degrees of heating after their formation, it is possible to date the timing of melt/core formation and thus provide constraints on when such objects must have formed. The primary tool used to study the formation ages of these objects has been the ^{182}Hf/^{182}W system (Kleine et al. 2009), as this system is based on elements that partition differently into the metallic core and silicate mantle during differentiation. That is, Hf is lithophile, meaning it has chemical affinities for silicates, whereas W is siderophile, meaning it will be incorporated into the metallic core when a planetesimal melts and differentiates. However, ^{182}Hf decays to ^{182}W on a timescale of 8.9 Myr, so any ^{182}Hf present in the silicate rocks after differentiation results in an excess of ^{182}W in the mantle (and a corresponding deficit in the metallic cores). This would be particularly true for early-formed bodies, as much ^{182}Hf would not have decayed and would remain in the mantles following differentiation.

Recent advances have allowed for high-precision measurements of ^{182}W in iron meteorites. Small variations are seen across different types of irons, but indications are that differentiation and core formation occurred over a period of ~1 Myr after CAI formation (Kleine et al. 2002, Burkhardt et al. 2008, Kruijer et al. 2014). Given the time required for ^{26}Al to heat a body to the point of melting and differentiation, the parent bodies of these iron meteorites must have formed only 0.1 to 0.3 Myr after CAI formation.

Thus, meteorite chronology indicates that planetesimal formation was not a singular event, but rather a protracted process in the solar nebula: Some bodies formed almost concurrently with CAIs, whereas others formed several millions of years later (**Figure 9**). Planetesimal formation models largely come in two types: (*a*) incremental accretion models where planetesimals form from continued collisions between dust grains and aggregates (Weidenschilling 1980, 1984; Weidenschilling et al. 1997) and (*b*) gravitational instability models where solids become spatially concentrated in the nebula through dynamical interactions with the gas to levels where they become gravitationally bound and contract to form a coherent body (Goldreich & Ward 1973; Cuzzi et al. 2001, 2008; Johansen et al. 2007). The merits and challenges to each model have recently been summarized from a dynamic perspective in Chiang & Youdin (2010). However, here we evaluate how these models fit with the meteoritic data.

The relatively old ages of iron meteorites indicate that planetesimal formation must have been rapid, allowing the submicrometer-sized dust grains suspended in the nebula to aggregate into objects that were many kilometers in radius on timescales of 10^5 years. However, the process by which planetesimals formed must have been inefficient, as fine dust, including presolar grains that escaped significant thermal processing, had to survive in the nebula for millions of years to allow the chondrite parent bodies to form at this later time. The same is true for CAIs: The fact that we see such objects means they must have avoided incorporation into planetesimals immediately after their formation. Otherwise, they would have been destroyed during the differentiation of the early-formed bodies.

Incremental accretion models predict that planetesimals could form rapidly, as required by the ages of iron meteorites, provided that sticking between the dust grains in collisions is efficient.

Astronomical timeline

Class II+III (disk lifetimes)

Class I

Class 0

$t = 0$ $t = 1$ Ma $t = 2$ Ma $t = 3$ Ma $t = 4$ Ma $t = 5$ Ma

CAI formation

Iron meteorite parent body accretion

Iron meteorite parent body differentiation

Chondrule formation

CB chondrite formation

Mars accretion

Cometary refractory inclusions formed

Extraterrestrial sample timeline

Figure 9

Comparison of the ATL (*top*) for the early stages of star and protoplanetary disk evolution with the ESTL (*bottom*) for our Solar System. Note that $t = 0$ is not necessarily the same in both timelines, but instead reflects the starting point for age estimates for each respective timeline. The ATL shows the stages of evolution for YSOs (Lada & Jugaku 1987, Andre et al. 1993), with Class 0 and Class I durations estimated by Evans et al. (2009) and Class II/III duration reported by Haisch et al. (2001). In all cases, these times represent median lifetimes (∼0.1, ∼0.4, and ∼3 Myr, respectively) estimated by classifying YSOs and estimating their ages. The ESTL shows the ages measured for distinct formation/processing events related to those described in the text. CAI and chondrule formation ages are Pb-Pb ages from Connelly et al. (2012). Note that CAI formation is thought to last only a brief period of time (<0.1 Myr), whereas chondrule formation is thought to have begun along with CAI formation and persisted for ∼3 Myr. Iron meteorite parent body formation and differentiation ages are taken from the Hf-W studies of Kruijer et al. (2014), who found such bodies must have accreted 0.1–0.3 Myr after CAIs with core formation lasting ∼1 Myr after CAI. CB chondrite formation is estimated to have taken place ∼5 Myr after the CAIs formed by Krot et al. (2005a) on the basis of ages of chondrules unique to that meteorite type; these ages may reflect an impact event and not necessarily a solar nebular process. The accretion time of Mars is taken from the Hf-W-Th studies of Martian meteorites by Dauphas & Pourmand (2011), who suggested that Mars accreted half its mass 0.8–2.7 Myr after CAIs formed. The ages of cometary refractory inclusions are inferred from $^{26}Al-^{26}Mg$ systematics of Coki, a refractory particle returned by the Stardust mission to comet Wild-2 (Matzel et al. 2010). Abbreviations: ATL, astronomical timeline; CAI, calcium-aluminum-rich inclusion; CB, Bencubbin-type carbonaceous chondrite subclass; ESTL, extraterrestrial sample timeline; Hf, hafnium; Pb, lead; Th, thorium; YSO, young stellar object; W, tungsten.

For example, Weidenschilling (1997) showed that growth in this way can produce bodies 1 km in radius on timescales of 10^5 years at distances of 30 AU in the solar nebula. The same processes would operate on even more rapid timescales closer to the young Sun, thus allowing potential iron meteorite parent bodies to form. However, when these large bodies form, they contain a large fraction of the mass of the solids; micrometer-sized dust is present at only approximately 1/1,000 the mass density of the kilometer-sized objects that form at the disk midplane. Determining

whether such a reduced population of small dust could survive for the needed period of time and could provide the raw materials to form chondrules and matrix in ways consistent with the meteoritic record requires further work. We especially need to determine the proportion of early-formed planetesimals to later-formed planetesimals in the early Solar System.

Gravitational instability models have gained traction in recent years with the recognition that collisional growth of dust as required by incremental accretion models can be difficult. That is, as dust grains aggregate into increasingly larger objects in the solar nebula, their collisional velocities also increase. These more energetic collisions stop being accretional and instead result in bouncing (no mass transfer) or are erosional (all resulting dust aggregates are smaller than the original colliding pair), thus frustrating growth (see review by Blum & Wurm 2008). Accordingly, growth via collisions would stall at sizes of centimeters to meters. This insight combined with the rapid inward drift of these particles due to gas drag leads to the problem of the meter-sized barrier, where growth via collisions beyond this size cannot occur (Weidenschilling 1977, Cuzzi et al. 2006). Gravitational instability models offer a means of leapfrogging this barrier by forming planetesimals in regions of the nebula where solids become spatially concentrated. Regions that become enhanced in solids could arise through the streaming instability (Johansen et al. 2007) or turbulent concentration (Cuzzi et al. 2001, 2008). Solids may also become concentrated in localized pressure gradients that arise from nonuniform evolution of the protoplanetary disk (e.g., Kretke & Lin 2007, Tan et al. 2015). Such regions could also prevent loss of solids via gas drag, with solids gathering as seen in dust traps in other protoplanetary disks (van der Marel et al. 2013).

Once these dense regions form, the solids begin to fall inward toward one another under the influence of gravity over timescales of tens to hundreds of orbital periods, thus allowing for rapid formation of planetesimals, consistent with the very old ages of iron meteorite parent bodies. Such high concentrations of solids may form infrequently in the disk, meaning that early formation of planetesimals left sufficient dust for later generations to form. Thus, in contrast to incremental accretion models, gravitational instability could allow for protracted formation of planetesimals from pristine nebular dust. Further work is needed to understand how dust growth develops to the point where such concentrations develop and how often these concentrations could arise in the disk. Although gravitational instability allows for rapid planetesimal formation, whether it will allow for fine dust to remain in a protoplanetary disk for millions of years remains unclear.

In summary, the diverse ages of meteorites and their components reveal that planetesimal formation was protracted, rather than occurring at one epoch of disk history. Planetesimal formation operated early but was not efficient, leaving significant amounts of dust suspended in the disk for millions of years. Thus, planetesimal properties and compositions reflect both spatial and temporal variations in the solar nebula.

5.3. Mixing and Transport in the Solar Nebula

Many aspects of meteorites and other extraterrestrial samples show that the solar nebula was a dynamic object. As described in Section 2, chondritic meteorites comprise a mix of components that record different formation environments in the solar nebula. That is, CAIs formed at high temperatures in a ^{16}O-rich reservoir, chondrules formed as a result of transient heating events in a ^{16}O-poor reservoir, and significant amounts of matrix materials remained cold, as they included relatively fragile presolar grains and organic materials that would have been destroyed in the CAI- and chondrule-forming regions, yet all these materials are intimately mixed on the scale of millimeters and centimeters. That such diverse materials, which record different nebular environments and histories, were brought together to be incorporated into common meteorite

parent bodies attests to the extent to which materials were redistributed within our protoplanetary disk.

Yet, although mixing and transport occurred, the nebula did not become perfectly chemically or isotopically homogenized. For example, continual technological improvements in recent years have allowed for characterization of an ever-expanding list of isotopic anomalies in various elements (e.g., Ca, Ti, Mo, Ba, Cr, osmium) seen at the scale of CAIs, bulk meteorites, and/or stepwise dissolution of bulk meteorites (Carlson et al. 2007 and references therein, Trinquier et al. 2009, Qin et al. 2010, Chen et al. 2011, Brennecka et al. 2013, Dauphas et al. 2014). These anomalies are for the most part substantially smaller than seen in individual presolar grains (Section 3), but their detectability at the bulk scale implies substantial heterogeneity in the distribution of carriers of different isotopic signatures in the solar nebula. This heterogeneity may be related to thermal processing and/or size sorting of different presolar phases in the nebula, but the details are still far from clear.

The notion of a dynamic solar nebula is consistent with our astrophysical understanding of protoplanetary disk evolution. Having formed as a result of angular momentum conservation within a collapsing cloud, most of the mass of a young star is incorporated into a disk and then transported inward to be accreted by the central object. This inward migration of material through the disk must be balanced by the outward transport of angular momentum, which may occur through internal processes that drive the radial expansion of the disk or as materials are carried away in winds along magnetic field lines.

Whether internal processes or disk winds are responsible for the physical evolution of protoplanetary disks remains the subject of ongoing research. Internal processes that might drive disk evolution include magnetorotational instability (MRI) (Balbus & Hawley 1991) and gravitational torques, each of which may operate in protoplanetary disks so long as certain conditions are met (Armitage 2011, Bai 2011, Bai & Stone 2013). For example, MRI requires sufficient ionization for disk materials to couple to magnetic fields, whereas gravitational torques are effective only in cool disks with sufficiently high surface densities (that is, massive compact disks). Magnetic field lines that thread the disk can carry materials away as collimated jets, e.g., the bipolar jets that seem to be ubiquitous within protoplanetary disks, though it is unclear whether such effects extend to disk interiors or are limited to the surface layers of the disk. Meteorites, however, provide a record of the magnetic fields of order 5–50 μT in the solar nebula (Fu et al. 2014), which may be used to evaluate disk evolution mechanisms.

Meteorites and other extraterrestrial materials allow us to gain insights into the extent of the dynamical evolution of our own solar nebula. Evidence for mixing is found in a variety of forms, but the samples the Stardust mission returned from the Jupiter-family (Kuiper Belt) comet Wild-2 have motivated most discussions in recent years (**Figure 2**) (Brownlee et al. 2006, Brownlee 2014). Among the ~0.001 g of material collected from the comet were refractory materials including crystalline olivine and grains rich in Ca and Al (Zolensky et al. 2006), whose chemistry is reminiscent of CAIs, as well as materials that resemble chondrule fragments (Nakamura et al. 2008). Further investigations demonstrated that these materials require high temperatures to form, similar to their chondritic counterparts and that their oxygen isotopic abundances were identical to those of materials found in chondritic meteorites (McKeegan et al. 2006, Nakamura et al. 2008). These observations pointed to a common origin for the chondritic and cometary materials, implying that these high-temperature materials were formed together and then mixed throughout the regions where these different types of bodies formed, e.g., the asteroid belt for chondrites and the trans-Neptunian region for Wild-2 (**Figure 2**).

To explain such formation and mixing, it is necessary to understand how solid materials would be redistributed within the solar nebula under the different evolutionary mechanisms outlined

above. Given internal processes like the MRI or gravitational instabilities, solid grains that formed in the inner regions of the solar nebula, where high temperatures are expected, can be carried outward as part of the radial expansion and random motions associated with disk evolution (Bockelée-Morvan et al. 2002, Cuzzi et al. 2003, Ciesla 2010, Boss 2012, Jacquet et al. 2012, Yang & Ciesla 2012). This transport would be most rapid and efficient early in disk evolution (the first few hundred thousand years) when disk accretion rates are highest, decaying away in importance and effectiveness during the later stages of disk history. In disk wind models, gas is carried upward and outward from the disk along magnetic field lines. If gas density is high enough and wind velocities rapid enough, small grains can get entrained in the flow (Safier 1993). However, as the gas moves away from the disk and becomes more rarefied, these grains will decouple from the flow at height and then rain back down on the disk again at greater distances than when they were launched.

Although both sets of models explain the outward transport of solids within a protoplanetary disk, they make different predictions about the dynamical behavior of volatiles. Internal processes predict that the solids and gas will be subjected to the same type of evolution, meaning that some fraction of the gas or volatiles in the outer regions of the protoplanetary disk will have originated from the hot inner regions of the disk. Disk wind models, however, predict that the gas will be separated from the dust—the gas will continue upward and away from the disk, whereas the solids rain back down onto the disk.

This difference is critical when we consider the water contained within primitive extraterrestrial materials. For example, the CI, CR (Renazzo type), and CM (Murray type) subclasses of carbonaceous chondrites (see sidebar Chondrite Classification) contain extensive evidence for aqueous alteration—that is, the reaction of water with rock to form hydrated and/or oxidized minerals such as serpentine, cronstedtite, and magnetite. The parent bodies of these meteorites must have formed when nebular water ice accreted with otherwise anhydrous rock; the ice then melted as a result of SLR heating, allowing the liquid water to react with the rock. As a result, the D/H ratio of the hydrated silicates found within these rocks reflects the D/H ratio of the nebular water ice that accreted into the parent planetesimals. Within chondrites, the D/H values for the hydrated silicates are similar to or lower than that found in Earth's oceans (1.5×10^{-4}) (Alexander et al. 2012). This value is significantly lower than the D/H value expected in interstellar water, which is estimated to fall in the range of 0.001–0.01 owing to ion-molecule chemistry and enhanced amounts of D reacting to form HDO on grain surfaces at low temperatures (Cleeves et al. 2014, Persson et al. 2014). The lower values in chondrites are the product of some of this interstellar water mixing with water that re-equilibrated with H_2 (with protosolar D/H of $\sim 2 \times 10^{-5}$) (Geiss & Gloeckler 2003) within the solar nebula. Such re-equilibration requires temperatures >500 K (Lecluse & Robert 1994, Yang et al. 2013); as a result, some chondritic water came from the warm regions of our protoplanetary disk. In fact, assuming a D/H value of 0.001 for interstellar water ice, 13% of the water in chondrites was inherited from the ISM, whereas the other 87% equilibrated at high temperatures in the disk—an even greater amount of equilibrated water is required if interstellar water began with a higher D/H value.

Comets from both the Oort Cloud and Kuiper Belt (**Figure 2**) also contain water with D/H values that are below the interstellar value (D/H ~ 1.5–5×10^{-4}), though these are determined through remote observations and not through extraterrestrial sample analysis (e.g., Hartogh et al. 2011, Altwegg et al. 2015). Given that water ice could be incorporated only into planetesimals (comets or hydrated asteroids) beyond the snow line (the region where temperatures were low enough for water to condense as ice, $T \lesssim 150$ K), the dominance of equilibrated water within chondrites and comets is suggestive of significant outward transport of gas in the solar nebula. Within the framework of disk evolution mechanisms described above, this outward transport is most efficient in internal disk evolutionary processes and less so in disk wind models.

Comparison of isotopic and chemical properties of grains in different parent bodies provides important insights into the extent to which planetary materials were shared across the early Solar System. The presence of similar materials in comets and chondritic meteorites suggests that mixing was significant in the solar nebula. Although the mechanisms responsible for this mixing remain uncertain, continued studies and comparison of the mixing that occurred for rocky and icy materials may help us to evaluate various models.

6. CONCLUDING REMARKS

As samples of the early Solar System and its original building blocks, meteorites, IDPs, and spacecraft-returned asteroidal and cometary fragments are very valuable resources for investigating a variety of astrophysical processes. In this review, we cover some important astrophysical applications of extraterrestrial materials analysis. Presolar stardust grains preserved in primitive materials provide direct laboratory probes of nucleosynthetic and dust formation processes in stars, GCE, and interstellar dust processing. Isotopic imprints of decay of short- and long-lived radioisotopes provide both clues about the astrophysical environment of our Solar System's birth and chronological information about processes in the earliest evolutionary stages of the protosolar disk. RIs and chondrules provide key constraints on the formation and processing of dust in the solar nebula. Furthermore, the intimate mixing of these high-temperature objects and low-temperature (volatile- and organic-rich fine-grained matrix) components in both asteroidal and cometary samples indicates that large-scale transport and mixing of materials occurred in our own protoplanetary disk and by extension in other disks as well. Finally, radiometric dating of chondrules and iron meteorites tell us about the timing and duration over which solar nebula solids were assembled into the building blocks of the planets.

However, the selective sampling of astrophysical applications of extraterrestrial materials presented here is hardly comprehensive. Owing to space limitations, we do not discuss additional interesting and important topics, which include the following:

1. The origin of the heterogeneity in O-isotopic ratios across the Solar System (**Figure 4a**), especially the 6% difference in ^{16}O abundance between the Sun and most bulk planetary materials: At present, a photochemical origin is popular (Clayton 2002, Yurimoto & Kuramoto 2004, Lyons & Young 2005), though the astrophysical setting is uncertain and other possible origins are still being discussed (Krot et al. 2010, Nittler & Gaidos 2012).

2. The origin of meteoritic organic matter, which is the dominant form of C in primitive solar system materials: H- and N-isotopic anomalies have long suggested an interstellar heritage for these materials (Messenger 2000, Busemann et al. 2006), but this has been challenged (e.g., Remusat et al. 2006). Thus, whether the organics are interstellar, nebular, and/or planetary in origin remains hotly debated (Alexander et al. 2010, Cody et al. 2011).

3. Irradiation processes in the Solar System: Young stars are prodigious producers of charged particles that will interact with protoplanetary disk materials (Feigelson et al. 2002), and even today, solar wind particles and galactic cosmic rays may interact with small bodies in interplanetary space. Isotopic, chemical, and/or microstructural imprints of these interactions recorded by extraterrestrial materials can thus shed light on the nature of the irradiation (e.g., energy spectrum), young star-disk interactions, and exposure history of materials prior to Earth delivery. Examples include perturbations in the isotopic ratios of light elements such as He, lithium, boron, and beryllium (Be) as well as evidence for the presence of live ^{10}Be (half-life = 1.4 Myr) in the early Solar System (McKeegan et al. 2000, Chaussidon & Gounelle 2006, Liu et al. 2010) and formation of nuclear tracks in crystals due to solar flare particles (Bradley & Brownlee 1986).

DISCLOSURE STATEMENT

The authors are not aware of any affiliations, memberships, funding, or financial holdings that might be perceived as affecting the objectivity of this review.

ACKNOWLEDGMENTS

LITERATURE CITED

Abia C, Isern J. 2000. *Ap. J.* 536:438–49

Alexander CMO'D. 2004. *Geochim. Cosmochim. Acta* 68:3943–69

Alexander CMO'D, Bowden R, Fogel ML, et al. 2012. *Science* 337:721–23

Alexander CMO'D, Grossman JN, Ebel DS, Ciesla FJ. 2008. *Science* 320:1617–19

Alexander CMO'D, Newsome SD, Fogel ML, et al. 2010. *Geochim. Cosmochim. Acta* 74:4417–37

Alexander CMO'D, Nittler LR. 1999. *Ap. J.* 519:222–35

Alexander CMO'D, Nittler LR, Ciesla FJ. 2014. *Meteorit. Planet. Sci.* 49(Suppl.):5241

Altwegg K, Balsiger H, Bar-Nun A, et al. 2015. *Science* 347(6220):1261952

Amari S, Gao X, Nittler LR, et al. 2001a. *Ap. J.* 551:1065–72

Amari S, Nittler LR, Zinner E, et al. 2001b. *Ap. J.* 559:463–83

Amari S, Zinner E, Gallino R. 2014. *Geochim. Cosmochim. Acta* 133:479–522

Amelin Y, Krot AN, Hutcheon ID, Ulyanov AA. 2002. *Science* 297:1678–83

Anders E, Zinner E. 1993. *Meteoritics* 28:490–514

Andre P, Ward-Thompson D, Barsony M. 1993. *Ap. J.* 406:122–41

Armitage PJ. 2011. *Annu. Rev. Astron. Astrophys.* 49:195–236

Asphaug E, Jutzi M, Movshovitz N. 2011. *Earth Planet. Sci. Lett.* 308:369–79

Asplund M, Lambert DL, Kipper T, et al. 1999. *Astron. Astrophys.* 343:507–18

Bai X-N. 2011. *Ap. J.* 739:50

Bai X-N, Stone JM. 2013. *Ap. J.* 769:76

Balbus SA, Hawley JF. 1991. *Ap. J.* 376:214–22

Bernatowicz TJ, Akande OW, Croat TK, Cowsik R. 2005. *Ap. J.* 631:988–1000

Bernatowicz TJ, Cowsik R, Gibbons PC, et al. 1996. *Ap. J.* 472:760–82

Beuther H, Klessen RS, Dullemond CP, Henning T, eds. 2014. *Protostars and Planets VI.* Tucson: Univ. Ariz. Press

Biscaro C, Cherchneff I. 2014. *Astron. Astrophys.* 564:A25

Blum J, Wurm G. 2008. *Annu. Rev. Astron. Astrophys.* 46:21–56

Bockelée-Morvan D, Gautier D, Hersant F, et al. 2002. *Astron. Astrophys.* 384:1107–18

Boley AC, Durisen RH. 2008. *Ap. J.* 685:1193–209

Boley AC, Morris MA, Desch SJ. 2013. *Ap. J.* 776:101

Boothroyd AI, Sackmann I-J. 1999. *Ap. J.* 510:232–50

Boss AP. 1998. *Annu. Rev. Earth Planet. Sci.* 26:53–80

Boss AP. 2012. *Annu. Rev. Earth Planet. Sci.* 40:23–43

Boss AP, Durisen RH. 2005. *Ap. J. Lett.* 621:L137–40

Boss AP, Keiser SA. 2015. *Ap. J.* 809:103

Bouvier A, Wadhwa M. 2010. *Nat. Geosci.* 3:637–41

Bradley JP, Brownlee DE. 1986. *Science* 231:1542–44

Brennecka GA, Borg LE, Wadhwa M. 2013. *PNAS* 110:17241–46

Brennecka GA, Weyer S, Wadhwa M, et al. 2010. *Science* 327:449–51

Brownlee D. 2014. *Annu. Rev. Earth Planet. Sci.* 42:179–205

Brownlee D, Tsou P, Aleon J, et al. 2006. *Science* 314:1711–16

Burbidge EM, Burbidge GR, Fowler WA, Hoyle F. 1957. *Rev. Mod. Phys.* 29:547–650

Burkhardt C, Kleine T, Bourdon B, et al. 2008. *Geochim. Cosmochim. Acta* 72:6177–97

Burnett DS. 2013. *Meteorit. Planet. Sci.* 48:2351–70

Busemann H, Young AF, Alexander CMO'D, et al. 2006. *Science* 312:727–30

Busso M, Wasserburg GJ, Nollett KM, Calandra A. 2007. *Ap. J.* 671:802–10

Cameron AGW. 1957. *Chalk River Rep. CRL-41*, Atomic Energy Can. Ltd.

Cameron AGW, Truran JW. 1977. *Icarus* 30:447–61

Carlson RW, Boyet M, Horan M. 2007. *Science* 316:1175–78

Chaussidon M, Gounelle M. 2006. See Lauretta & McSween Jr. 2006, pp. 323–39

Chen H-W, Lee T, Lee D-C, et al. 2011. *Ap. J. Lett.* 743:L23

Chiang E, Youdin AN. 2010. *Annu. Rev. Earth Planet. Sci.* 38:493–522

Ciesla FJ. 2010. *Icarus* 208:455–67

Clayton DD. 1983. *Ap. J.* 268:381–84

Clayton DD. 1988. *Ap. J.* 334:191–95

Clayton DD. 1997. *Ap. J. Lett.* 484:L67–70

Clayton DD. 2003. *Ap. J.* 598:313–24

Clayton DD. 2013. *Ap. J.* 762:5

Clayton DD, Arnett D, Kane J, Meyer BS. 1997. *Ap. J.* 486:824–34

Clayton DD, Deneault EA-N, Meyer BS. 2001. *Ap. J.* 562:480–93

Clayton DD, Liu W, Dalgarno A. 1999. *Science* 283:1290–92

Clayton DD, Timmes FX. 1997. *Ap. J.* 483:220–27

Clayton RN. 2002. *Nature* 415:860–61

Clayton RN, Grossman L, Mayeda TK. 1973. *Science* 182:485–88

Cleeves LI, Bergin EA, Alexander CMO'D, et al. 2014. *Science* 345:1590–93

Cody GD, Heying E, Alexander CMO'D, et al. 2011. *PNAS* 108:19171–76

Connelly JN, Bizzaro M, Krot AN, et al. 2012. *Science* 338:651–55

Connolly HC Jr., Desch SJ. 2004. *Chem. Erde/Geochem.* 64:95–125

Cristallo S, Piersanti L, Straniero O, et al. 2011. *Ap. J. Suppl.* 197:17

Croat TK, Bernatowicz T, Amari S, et al. 2003. *Geochim. Cosmochim. Acta* 67:4705–25

Croat TK, Stadermann FJ, Bernatowicz TJ. 2005. *Ap. J.* 631:976–87

Cuzzi JN, Alexander CMO'D. 2006. *Nature* 441:483–85

Cuzzi JN, Davis SS, Dobrovolskis AR. 2003. *Icarus* 166:385–402

Cuzzi JN, Hogan RC, Paque JM, Dobrovolskis AR. 2001. *Ap. J.* 546:496–508

Cuzzi JN, Hogan RC, Shariff K. 2008. *Ap. J.* 687:1432–47

Cuzzi JN, Weidenschilling SJ, McSween HY. 2006. See Lauretta & McSween Jr. 2006, pp. 353–81

D'Alessio P, Calvet N, Woolum DS. 2005. See Krot et al. 2005b, pp. 353–72

Dai ZR, Bradley JP, Joswiak DJ, et al. 2002. *Nature* 418:157–59

Daulton TL, Bernatowicz TJ, Lewis RS, et al. 2002. *Science* 296:1852–55

Dauphas N, Chaussidon M. 2011. *Annu. Rev. Earth Planet. Sci.* 39:351–86

Dauphas N, Chen JH, Zhang J, et al. 2014. *Earth Planet. Sci. Lett.* 407:96–108

Dauphas N, Pourmand A. 2011. *Nature* 473:489–92

Dauphas N, Remusat L, Chen JH, et al. 2010. *Ap. J.* 720:1577–91

Davis AM, ed. 2014. *Meteorites and Cosmochemical Processes: Treatise on Geochemistry*, Vol. 1. Oxford: Elsevier-Pergamon. 2nd ed.

Davis AM, Alexander CMO'D, Nagahara H, Richter FM. 2005. See Krot et al. 2005b, pp. 432–55

Davis AM, McKeegan KD. 2014. See Davis 2014, pp. 361–95

Deneault EA-N, Clayton DD, Heger A. 2003. *Ap. J.* 594:312–25

Denissenkov PA, Tout CA. 2003. *MNRAS* 340:722–32

Desch SJ, Morris MA, Connolly HC, Boss AP. 2012. *Meteorit. Planet. Sci.* 47:1139–56

Draine BT. 1990. In *The Evolution of the Interstellar Medium*, ed. L Blitz, *ASP Conf. Ser.* 12:193–205. San Francisco: ASP

Draine BT. 2009. In *Cosmic Dust: Near and Far*, ed. T Henning, E Grün, J Steinacker, *ASP Conf. Ser.* 414:453–72. San Francisco: ASP

Dullemond CP, Stammler SM, Johansen A. 2014. *Ap. J.* 794:91

Ebel DS. 2006. See Lauretta & McSween Jr. 2006, pp. 253–77

Evans NJ II, Dunham MM, Jørgensen JK, et al. 2009. *Ap. J. Suppl.* 181:321–50

Fedkin AV, Grossman L, Ciesla FJ, Simon SB. 2012. *Geochim. Cosmochim. Acta* 87:81–116

Feigelson ED, Garmire GP, Pravdo SH. 2002. *Ap. J.* 572:335–49

Floss C, Stadermann FJ, Bose M. 2008. *Ap. J.* 672:1266–71

Foster PN, Boss AP. 1997. *Ap. J.* 489:346–57

Freiburghaus C, Rosswog S, Thielemann F-K. 1999. *Ap. J. Lett.* 525:L121–24

Fu RR, Weiss BP, Lima EA, et al. 2014. *Science* 346:1089–92

Fujiya W, Hoppe P, Zinner E, et al. 2013. *Ap. J. Lett.* 776:L29

Gaidos E, Krot AN, Williams JP, Raymond SN. 2009. *Ap. J.* 696:1854–63

Gail H-P, Sedlmayr E. 1999. *Astron. Astrophys.* 347:594–616

Gail H-P, Zhukovska SV, Hoppe P, Trieloff M. 2009. *Ap. J.* 698:1136–54

Gal-Yam A, Arcavi I, Ofek EO, et al. 2014. *Nature* 509:471–74

Gall C, Hjorth J, Watson D, et al. 2014. *Nature* 511:326–29

Gallino R, Arlandini C, Busso M, et al. 1998. *Ap. J.* 497:388–403

Geiss J, Gloeckler G. 2003. *Space Sci. Rev.* 106:3–18

Goldreich P, Ward WR. 1973. *Ap. J.* 183:1051–62

Gounelle M, Meibom A, Hennebelle P, Inutsuka S-I. 2009. *Ap. J. Lett.* 694:L1–L5

Gounelle M, Meynet G. 2012. *Astron. Astrophys.* 545:4

Groopman E, Bernatowicz T, Zinner E. 2012. *Ap. J. Lett.* 754:L8

Groopman E, Bernatowicz T, Zinner E, Nittler LR. 2014. *Ap. J.* 790:9

Grossman L. 1972. *Geochim. Cosmochim. Acta* 36:597–619

Gyngard F, Amari S, Zinner E, Ott U. 2009. *Ap. J.* 694:359–66

Gyngard F, Nittler LR, Zinner E, et al. 2011. *Proc. Lunar Planet. Sci. Conf.*, *42nd*, The Woodlands, TX, Abstr. 2675

Gyngard F, Nittler LR, Zinner EK, Jose J. 2010a. *Proc. Symp. Nuclei Cosmos*, 11th, Heidelberg, Ger., p. 141

Gyngard F, Zinner E, Nittler LR, et al. 2010b. *Ap. J.* 717:107–20

Haisch KE Jr., Lada EA, Lada CJ. 2001. *Ap. J. Lett.* 553:L153–L56

Hammer NJ, Janka H-T, Müller E. 2010. *Ap. J.* 714:1371–85

Hartogh P, Lis DC, Bockelée-Morvan D, et al. 2011. *Nature* 478:218–20

Heck PR, Amari S, Hoppe P, et al. 2009a. *Ap. J.* 701:1415–25

Heck PR, Gyngard F, Ott U, et al. 2009b. *Ap. J.* 698:1155–64

Heck PR, Marhas KK, Hoppe P, et al. 2007. *Ap. J.* 656:1208–22

Hedrosa RP, Abia C, Busso M, et al. 2013. *Ap. J. Lett.* 768:L11

Henning T. 2010. *Annu. Rev. Astron. Astrophys.* 48:21–46

Herwig F, Pignatari M, Woodward PR, et al. 2011. *Ap. J.* 727:89

Hewins RH, Zanda B, Bendersky C. 2012. *Geochim. Cosmochim. Acta* 78:1–17

Höfner S. 2008. *Astron. Astrophys.* 491:L1–L4

Hoppe P, Strebel R, Eberhardt P, et al. 2000. *Meteorit. Planet. Sci.* 35:1157–76

Huss GR, Meyer BS, Srinivasan G, et al. 2009. *Geochim. Cosmochim. Acta* 73:4922–45

Hynes KM, Croat TK, Amari S, et al. 2010. *Meteorit. Planet. Sci.* 45:596–614

Indebetouw R, Matsuura M, Dwek E, et al. 2014. *Ap. J. Lett.* 782:L2

Jacobsen B, Yin Q-Z, Moynier F, et al. 2008. *Earth Planet. Sci. Lett.* 272:353–64

Jacobsen SB. 2005. See Krot et al. 2005b, pp. 548–57

Jacquet E, Gounelle M, Fromang S. 2012. *Icarus* 220:162–73

Jadhav M, Amari S, Marhas KK, et al. 2008. *Ap. J.* 682:1479–85

Jadhav M, Pignatari M, Herwig F, et al. 2013. *Ap. J. Lett.* 777:L27

Joggerst CC, Almgren A, Woosley SE. 2010. *Ap. J.* 723:353–63

Johansen A, Oishi JS, Mac Low M-M, et al. 2007. *Nature* 448:1022–25

Johnson BC, Minton DA, Melosh HJ, Zuber MT. 2015. *Nature* 517:339–41

Jones AP, Nuth JA. 2011. *Astron. Astrophys.* 530:A44

Jones AP, Tielens AGGM, Hollenbach DJ. 1996. *Ap. J.* 469:740–64

Jones AP, Tielens AGGM, Hollenbach DJ, McKee CF. 1997. In *Astrophysical Implications of the Laboratory Study of Presolar Materials*, ed. TJ Bernatowicz, E Zinner, *AIP Conf. Ser.* 402:595–613. St. Louis, MO: AIP

Jones OC, Kemper F, Sargent BA, et al. 2012. *MNRAS* 427:3209–29

Jones OC, Kemper F, Srinivasan S, et al. 2014. *MNRAS* 440:631–51

José J, Hernanz M, Amari S, et al. 2004. *Ap. J.* 612:414–28

Käppeler F, Gallino R, Busso M, et al. 1990. *Ap. J.* 354:630–43

Keller LP, Messenger S. 2011. *Geochim. Cosmochim. Acta* 75:5336–65

Kemper F, Vriend WJ, Tielens AGGM. 2004. *Ap. J.* 609:826–37

Kinoshita N, Paul M, Kashiv Y, et al. 2012. *Science* 335:1614–17

Kita NT, Huss GR, Tachibana S, et al. 2005. See Krot et al. 2005b, pp. 558–87

Kleine T, Münker C, Mezger K, Palme H. 2002. *Nature* 418:952–55

Kleine T, Touboul M, Bourdon B, et al. 2009. *Geochim. Cosmochim. Acta* 73:5150–88

Kobayashi C, Karakas AI, Umeda H. 2011. *MNRAS* 414:3231–50

Koehler P, Harvey JA, Guber K, Wiarda DA. 2008. *Proc. Symp. Nuclei Cosmos*, *10th*, Mackinac Island, MI, p. 41

Kretke KA, Lin DNC. 2007. *Ap. J. Lett.* 664:L55–58

Krot AN, Amelin Y, Cassen P, Meibom A. 2005a. *Nature* 436:989–92

Krot AN, Nagashima K, Ciesla FJ, et al. 2010. *Ap. J.* 713:1159–66

Krot AN, Scott ERD, Reipurth B, eds. 2005b. *Chondrites and the Protoplanetary Disk*, *ASP Conf. Ser.*, Vol. 341. San Francisco: ASP

Krot AN, Yurimoto H, Hutcheon ID, MacPherson GJ. 2005c. *Nature* 434:998–1001

Kruijer TS, Kleine T, Fischer-Gödde M, et al. 2014. *Earth Planet. Sci. Lett.* 403:317–27

Lada CJ, Jugaku J. 1987. In *Star Forming Regions*, ed. M Peimbert, J Jugaku, Int. Astron. Union Symp., pp. 1–17. New York: Springer

Lauretta DS, McSween HY Jr., eds. 2006. *Meteorites and the Early Solar System II*. Tucson: Univ. Ariz. Press

Lecluse C, Robert F. 1994. *Geochim. Cosmochim. Acta* 58:2927–40

Lee T, Papanastassiou DA, Wasserburg GJ. 1976. *Geophys. Res. Lett.* 3:109–12

Lee T, Papanastassiou DA, Wasserburg GJ. 1977. *Ap. J. Lett.* 211:L107–10

Leitner J, Kodolányi J, Hoppe P, Floss C. 2012. *Ap. J. Lett.* 754:L41

Lewis RS, Tang M, Wacker JF, et al. 1987. *Nature* 326:160–62

Lin Y, Gyngard F, Zinner E. 2010. *Ap. J.* 709:1157–73

Liu M-C. 2014. *Ap. J. Lett.* 781:L28

Liu M-C, Chaussidon M, Srinivasan G, McKeegan KD. 2012. *Ap. J.* 761:137

Liu M-C, Nittler LR, Alexander CMO'D, Lee T. 2010. *Ap. J. Lett.* 719:L99–103

Liu N, Gallino R, Bisterzo S, et al. 2014a. *Ap. J.* 788:163

Liu N, Savina MR, Davis AM, et al. 2014b. *Ap. J.* 786:66

Liu N, Nittler LR, Alexander CMO'D, et al. 2016. *Ap. J.* 820(2):140

Lugaro M, Davis AM, Gallino R, et al. 2003. *Ap. J.* 593:486–508

Lugaro M, Heger A, Osrin D, et al. 2014. *Science* 345:650–53

Lugaro M, Zinner E, Gallino R, Amari S. 1999. *Ap. J.* 527:369–94

Lyons JR, Young ED. 2005. *Nature* 435:317–20

MacPherson GJ, Davis AM, Zinner EK. 1995. *Meteoritics* 30:365–86

MacPherson GJ, Wark DA, Armstrong JT. 1988. In *Meteorites and the Early Solar System*, ed. JF Kerridge, MS Matthews, pp. 746–807. Tucson: Univ. Ariz. Press

Marhas KK, Amari S, Gyngard F, et al. 2008. *Ap. J.* 689:622–45

Marvin UB. 1995. *Meteoritics* 30:540–41

Matsuura M, Dwek E, Meixner M, et al. 2011. *Science* 333:1258–61

Matteucci F. 2003. *The Chemical Evolution of the Galaxy*. Dordrecht, Ger.: Kluwer Acad.

Matzel JEP, Ishii HA, Joswiak D, et al. 2010. *Science* 328:483–86

McCoy TJ, Robinson MS, Nittler LR, Burbine TH. 2002. *Chem. Erde* 62:89–121

McKeegan KD, Aleon J, Bradley J, et al. 2006. *Science* 314:1724–28

McKeegan KD, Chaussidon M, Robert F. 2000. *Science* 289:1334–37

McKeegan KD, Kallio APA, Heber VS, et al. 2011. *Science* 332:1528–32

McWilliam A. 1997. *Annu. Rev. Astron. Astrophys.* 35:503–56

Messenger S. 2000. *Nature* 404:968–71

Messenger S, Keller LP, Lauretta DS. 2005. *Science* 309:737–41

Messenger S, Keller LP, Stadermann FJ, et al. 2003. *Science* 300:105–8

Meyer BS. 1994. *Annu. Rev. Astron. Astrophys.* 32:153–90

Meyer BS, Bojazi MJ, The L-S, El Eid MF. 2011. *Meteorit. Planet. Sci.* 74(Suppl.):5457

Meyer BS, Clayton DD, The L-S. 2000. *Ap. J. Lett.* 540:L49–52

Morris MA, Boley AC, Desch SJ, Athanassiadou T. 2012. *Ap. J.* 752:27

Nakamura T, Noguchi T, Tanaka M, et al. 2011. *Science* 333:1113–16

Nakamura T, Noguchi T, Tsuchiyama A, et al. 2008. *Science* 321:1664–67

Nesvorný D, Jenniskens P, Levison HF, et al. 2010. *Ap. J.* 713:816–36

Nguyen AN, Keller LP, Rahman Z, Messenger S. 2011. *Meteorit. Planet. Sci.* 74(Suppl.):5449

Nguyen AN, Messenger S. 2014. *Ap. J.* 784:149

Nguyen AN, Nittler LR, Stadermann FJ, et al. 2010. *Ap. J.* 719:166–89

Nguyen AN, Stadermann FJ, Zinner E, et al. 2007. *Ap. J.* 656:1223–40

Nittler LR. 2005. *Ap. J.* 618:281–96

Nittler LR. 2009. *Pub. Astron. Soc. Aust.* 26:271–77

Nittler LR. 2013. *Meteorit. Planet. Sci.* 48(Suppl.):5144

Nittler LR, Alexander CMO'D. 2003. *Geochim. Cosmochim. Acta* 67:4961–80

Nittler LR, Alexander CMO'D, Gallino R, et al. 2008. *Ap. J.* 682:1450–78

Nittler LR, Alexander CMO'D, Gao X, et al. 1997. *Ap. J.* 483:475–95

Nittler LR, Amari S, Zinner E, et al. 1996. *Ap. J. Lett.* 462:L31–34

Nittler LR, Cowsik R. 1997. *Phys. Rev. Lett.* 78:175–78

Nittler LR, Dauphas ND. 2006. See Lauretta & McSween Jr. 2006, pp. 127–46

Nittler LR, Gaidos E. 2012. *Meteorit. Planet. Sci.* 47:2031–48

Nittler LR, Hoppe P. 2005. *Ap. J. Lett.* 631:L89–L92

Nittler LR, Hoppe P, Stroud RM. 2007. *Proc. Lunar Planet. Sci. Conf.*, *38th*, League City, TX, Abstr. 2321

Nollett KM, Busso M, Wasserburg GJ. 2003. *Ap. J.* 582:1036–58

Norris BRM, Tuthill PG, Ireland MJ, et al. 2012. *Nature* 484:220–22

Nozawa T, Kozasa T, Habe A, et al. 2007. *Ap. J.* 666:955–66

Nucci MC, Busso M. 2014. *Ap. J.* 787:141

Ott U, Begemann F. 2000. *Meteorit. Planet. Sci.* 35:53–63

Ouellette N, Desch SJ, Hester JJ. 2007. *Ap. J.* 662:1268–81

Pagel BEJ. 1997. *Nucleosynthesis and Chemical Evolution of Galaxies*. Cambridge, UK: Cambridge Univ. Press

Palme H, Hezel DC, Ebel DS. 2015. *Earth Planet. Sci. Lett.* 411:11–19

Palmerini S, La Cognata M, Cristallo S, Busso M. 2011. *Ap. J.* 729:3

Pan L, Desch SJ, Scannapieco E, Timmes FX. 2012. *Ap. J.* 756:102

Persson MV, Jørgensen JK, van Dishoeck EF, Harsono D. 2014. *Astron. Astrophys.* 563:74

Pettini M, Smith LJ, Hunstead RW, King DL. 1994. *Ap. J.* 426:79–96

Pignatari M, Wiescher M, Timmes FX, et al. 2013a. *Ap. J. Lett.* 767:L22

Pignatari M, Zinner E, Bertolli MG, et al. 2013b. *Ap. J. Lett.* 771:L7

Pignatari M, Zinner E, Hoppe P, et al. 2015. *Ap. J. Lett.* 808:L43

Podosek FA. 1970. *Earth Planet. Sci. Lett.* 8:183–87

Preibisch T, Brown AGA, Bridges T, Guenther E, Zinnecker H. 2002. *Astron. J.* 124:404–16

Qin L, Alexander CMO'D, Carlson RW, et al. 2010. *Geochim. Cosmochim. Acta* 74:1122–45

Qin L, Nittler LR, Alexander CMO'D, et al. 2011. *Geochim. Cosmochim. Acta* 75:629–44

Rauscher T, Heger A, Hoffman RD, Woosley SE. 2002. *Ap. J.* 576:323–48

Remusat L, Palhol F, Robert F, et al. 2006. *Earth Planet. Sci. Lett.* 243:15–25

Reynolds JH. 1960. *Phys. Rev. Lett.* 4:351–54

Reynolds JH, Turner G. 1964. *J. Geophys. Res.* 69:3263–81

Rho J, Kozasa T, Reach WT, et al. 2008. *Ap. J.* 673:271–82

Rotundi A, Baratta GA, Borg J, et al. 2008. *Meteorit. Planet. Sci.* 43:367–97

Rugel G, Faestermann T, Knie K, et al. 2009. *Phys. Rev. Lett.* 103:72502

Safier PN. 1993. *Ap. J.* 408:115–59

Sakamoto N, Seto Y, Itoh S, et al. 2007. *Science* 317:231–33

Savina MR, Davis AM, Tripa CE, et al. 2004. *Science* 303:649–52

Savina MR, Tripa CE, Pellin MJ, et al. 2003. *Proc. Lunar Planet. Sci. Conf.*, *34th*, League City, TX, Abstr. 2079

Schramm DN, Wasserburg GJ. 1970. *Ap. J.* 162:57–69

Scott ERD. 2007. *Annu. Rev. Earth Planet. Sci.* 35:577–620

Scott ERD, Krot AN. 2005. In *Treatise on Geochemistry*, Vol. 1: *Meteorites, Comets and Planets*, ed. AM Davis, pp. 143–200. Oxford, UK: Elsevier- Pergamon

Seab CG, Shull JM. 1983. *Ap. J.* 275:652–60

Sengupta S, Izzard RG, Lau HHB. 2013. *Astron. Astrophys.* 559:66

Silvia DW, Smith BD, Shull JM. 2010. *Ap. J.* 715:1575–90

Smith VV, Lambert DL. 1990. *Ap. J. Suppl.* 72:387–416

Speck AK, Barlow MJ, Skinner CJ. 1997. *MNRAS* 288:431–56

Stadermann FJ, Croat TK, Bernatowicz TJ, et al. 2005. *Geochim. Cosmochim. Acta* 69:177–88

Stammler SM, Dullemond CP. 2014. *Icarus* 242:1–10

Stroud RM, Chisholm MF, Heck PR, et al. 2011. *Ap. J. Lett.* 738:L27

Stroud RM, De Gergorio BT, Nittler LR, Alexander CMO'D. 2014. *Proc. Lunar Planet. Sci. Conf.*, *45th*, The Woodlands, TX, Abstr. 2806

Stroud RM, Nittler LR, Alexander CMO'D. 2004a. *Science* 305:1455–57

Stroud RM, Nittler LR, Alexander CMO'D. 2006. *Meteorit. Planet. Sci.* 41(Suppl.):5360

Stroud RM, Nittler LR, Alexander CMO'D. 2013. *Proc. Lunar Planet. Sci. Conf.*, *44th*, The Woodlands, TX, Abstr. 2315

Stroud RM, Nittler LR, Hoppe P. 2004b. *Meteorit. Planet. Sci.* 39(Suppl.):5039

Takigawa A, Stroud RM, Nittler LR, et al. 2014. *Proc. Lunar Planet. Sci. Conf.*, *45th*, The Woodlands, TX, Abstr. 1465

Tan JC, Chatterjee S, Hu X, Zhu Z, Mohanty S. 2015. In *Proc. 29th IAU GA Focus Meet. 1: Dynamical Problems in Extrasolar Planets Sci.*, ed. A Morbidelli, et al. In press. arXiv:1510.06703

Tang H, Dauphas N. 2012. *Earth Planet. Sci. Lett.* 359:248–63

Timmes FX, Clayton DD. 1996. *Ap. J.* 472:723–41

Timmes FX, Woosley SE, Weaver TA. 1995. *Ap. J. Suppl.* 98:617–58

Tinsley BM. 1977. *Ap. J.* 216:548–59

Tinsley BM. 1980. *Fundam. Cosmic Phys.* 5:287–388

Travaglio C, Gallino R, Amari S, et al. 1999. *Ap. J.* 510:325–54

Trinquier A, Elliott T, Ulfbeck D, et al. 2009. *Science* 324:374–76

van der Marel N, van Dishoeck EF, Bruderer S, et al. 2013. *Science* 340:1199–202

Vollmer C, Brenker FE, Hoppe P, Stroud RM. 2009. *Ap. J.* 700:774–82

Vollmer C, Hoppe P, Brenker FE. 2013. *Ap. J.* 769:61

Vollmer C, Hoppe P, Brenker FE, Holzapfel C. 2007. *Ap. J. Lett.* 666:L49–L52

Voss F, Wisshak K, Guber K, et al. 1994. *Phys. Rev. C* 50:2582–602

Wanajo S, Janka H-T, Müller B. 2011. *Ap. J. Lett.* 726:L15

Wasserburg GJ, Boothroyd AI, Sackmann I-J. 1995. *Ap. J. Lett.* 447:L37–40

Wasserburg GJ, Busso M, Gallino R, Nollett KM. 2006. *Nucl. Phys. A* 777:5–69

Weidenschilling SJ. 1980. *Icarus* 44:807–9

Weidenschilling SJ. 1984. *Icarus* 60:553–67

Weidenschilling SJ. 1997. In *From Stardust to Planetesimals*, ed. YJ Pendleton, AGGM Tielens, *ASP Conf. Ser.* 122:281–93. San Francisco: ASP

Weidenschilling SJ, Spaute D, Davis DR, et al. 1997. *Icarus* 128:429–55

Weidenschilling SW. 1977. *MNRAS* 180:57–70

Whittet DCB. 2002. *Dust in the Galactic Environment.* Bristol, UK: Inst. Phys.

Winteler C, Käppeli R, Perego A, et al. 2012. *Ap. J. Lett.* 750:L22

Yang L, Ciesla FJ. 2012. *Meteorit. Planet. Sci.* 47:99–119

Yang L, Ciesla FJ, Alexander CMO'D. 2013. *Icarus* 226:256–67

Young ED. 2014. *Earth Planet. Sci. Lett.* 392:16–27

Yurimoto H, Kuramoto K. 2004. *Science* 305:1763–66

Zega TJ, Alexander CMO'D, Nittler LR, Stroud RM. 2011. *Ap. J.* 730:83–92

Zega TJ, Haenecour P, Floss C, Stroud RM. 2015. *Ap. J.* 808:55

Zega TJ, Nittler LR, Gyngard F, et al. 2014. *Geochim. Cosmochim. Acta* 124:152–69

Zhang X, Jeffery CS. 2013. *MNRAS* 430:2113–20

Zhukovska S, Gail HP, Trieloff M. 2008. *Astron. Astrophys.* 479:453–80

Zinner E. 2014. See Davis 2014, pp. 181–213

Zinner E, Jadhav M, Gyngard F, Nittler LR. 2011. *Proc. Lunar Planet. Sci. Conf.*, *42nd*, The Woodlands, TX, Abstr. 1070

Zolensky ME, Zega TJ, Yano H, et al. 2006. *Science* 314:1735–39

**Annual Review of
Astronomy and
Astrophysics**

Volume 54, 2016

Contents

Indexes

Errata

An online log of corrections to *Annual Review of Astronomy and Astrophysics* articles
may be found at http://www.annualreviews.org/errata/astro